Florian Kleinegger, BSc.

Role of ID-1 in “cancer stem-cell-ness” of the gastroenteropancreatic neuroendocrine tumor cell line P-STS

MASTERARBEIT

Zur Erlangung des akademischen Grades

Master of Science

Masterstudium Biochemie und Molekulare Biomedizin

eingereicht an der

Technischen Universität Graz

Betreuer

Ao.Univ.-Prof. i.R. Dr. phil. Roswitha Pfragner
Univ.-Ass. Mag. Dr. Nassim Ghaffari Tabrizi-Wizsy

Institut für Pathophysiologie und Immunologie
Medizinische Universität Graz

Graz, August 2015

EIDESSTATTLICHE ERKLÄRUNG

Ich erkläre an Eides statt, dass ich die vorliegende Arbeit selbstständig verfasst, andere als die angegebenen Quellen/Hilfsmittel nicht benutzt, und die den benutzten Quellen wörtlich und inhaltlich entnommene Stellen als solche kenntlich gemacht habe. Das in TUGRAZonline hochgeladene Textdokument ist mit der vorliegenden Masterarbeit identisch.

…… ……..

Datum Unterschrift

Acknowledgement

First of all, I want to thank my supervisor Nassim Ghaffari Tabrizi-Wizsy who has given me the opportunity to write my master thesis in her research group. During my work, she always pushed me forward, taught me rare techniques and beyond that, made it possible for me to attend several conferences as a master student. I will always remember our good times in Barcelona.

Special thanks to Roswitha Pfragner and Gert Schwach for giving me the possibility to work with a neuroendocrine tumor cell line and their many advices in cell culture and tumor biology.

I appreciated working at the Institute of Pathophysiology and Immunology, where I met awesome people, who I call friends rather than colleagues.

Nathalie, Anika, Waltraud, Karin and Robert thank you for giving me technical support and lively discussions.

Carmen, what would I have done without you helping me wherever and whenever you could? I will always remember our nice jogging tours with Nicole and Martina hoping that they continue in future (and probably that Nicole will reduce her pace a little bit).

Corinna, Christina, Ruben and Izabela thank you for sharing the office with me. I always enjoyed having you around, especially our nice get-togethers after work. Thank you for trying to help me with all my tiny problems.

Pez, what should I say? I don't know how to thank you for supporting me, helping me with my works, forcing me to write, correcting my thesis and beyond that having a shoulder for me to rest on. You mean so much to me.

Many thanks to all of my friends for the nice discussions, distractions and for being part of my life.

And last but not least, Mum, thank you for everything.

"… if a biologist can think of a molecular mechanism, the cell is probably already using it."

Robert Benezra, Trends in Cell Biology (2003)

Table of content

Abbreviations

APS	Ammoniumpersulfate
ATF3	Activating of transcription factor 3
BAN	4-Bromoanisole
BB	Backbone (control of ID-1 overexpression)
BCA	Bicinchoninic acid
bFGF	Basic fibroblast growth factor
bHLH	Basic helix-loop-helix
BMP	Bone morphogenic protein
bp	Base pairs
BSA	Bovine serum albumin
CAM	Chicken chorioallantoic membrane
CDK	Cyclin-dependent kinase
CMF	Calcium and magnesium free
Cq	Cycle of quantity
CSC	Cancer stem cell
DAPI	2-(4-Amidinophenyl)-1*H*-indole-6-carboxamidine
DMEM	Dulbecco's modified eagle medium
ECL	Enhanced chemiluminescence
EGF	Epidermal growth factor
EGR-1	Early growth response protein 1
E-proteins	Ubiquitously expressed proteins
ETS	E26 transformation-specific
FACS	Flow activated cell sorting
FBS	Fetal bovine serum
fwd	Forward
GEP	Gastroenteropancreatic
GFP	Green fluorescent protein
HLH	Helix-loop-helix
HRP	Horseradish peroxidase
ID	Inhibitor of differentiation/DNA binding
IF	Immunofluorescence
IHC	Immunohistochemistry
LB	Lysogeny broth
M199	Medium 199
MMP2	Matrix metalloprotease 2
MTC	Medullary thyroid carcinoma
NET	Neuroendocrine tumor
NTC	No template control
P/S	Penicillin/Streptomycin
Pac	Puromycin *N*-acetyltransferase
PAGE	Polyacrylamide gel electrophoresis
PAI	Plasminogen activator inhibitor
PBS	Phosphate buffered saline
PFA	Paraformaldehyde (Polyoxymethylene)
PVDF	Poly(1,1-difluoroethylene)
qPCR	Quantitative PCR
Rb	Retinoblastoma proteins

rev	Reverse
RFU	Relative fluorescence unit
RT	Reverse transcriptase
S.O.C	Super optimal broth with catabolite repression
SBE	Smad-binding elements
scr	Scrambled (control of silencing constructs)
SDS	Sodiumdodecylsulfate
SEM	Standard error of mean
siA	siRNA version A
siB	siRNA version B
TBS-T	TRIS-buffered saline with Tween-20
TEMED	*N*,*N*,*N*',*N*'-Tetramethylethane-1,2-diamine
TF	Transcription factor
TGFβ	Transforming growth factor β
TRIS	2-Amino-2-(hydroxymethyl)-propane-1,3-diol
WST-1	Water soluble tetrazolium salts

List of tables

List of figures

Zusammenfassung

Einleitung: ID-1 wurde als erstes von vier Mitgliedern der Proteinfamilie „Inhibiton of DNA binding“ (ID) identifiziert. ID Proteine bestehen aus einer Helix-Loop-Helix Struktur (HLH), welche selbst keine DNA Bindesequenz hat, aber mit basic HLH (bHLH) Transkriptionsfaktoren interagiert und deren Bindung an die DNA beeinflusst. Es ist bekannt, dass ID-1 in über 20 verschieden Krebsarten, u.a. dem medullären Schilddrüsenkarzinom, welches zur Gruppe der neuroendokrinen Tumore (NET) gezählt wird, verstärkt vorhanden ist. Außerdem wurde ID-1 als Stammzellmarker in normalen und malignen Zellen beschrieben. In unserer Arbeitsgruppe wurde die Anwesenheit von Krebsstammzellen (CSC) in der gastroentero-pankreatischen NET Zelllinie P-STS gezeigt. Zusätzlich weisen P-STS Zellen, die in 3D-Kultur wachsen eine fünffach höhere Expression von ID-1 gegenüber Zellen in 2D-Kultur auf. Diese Beobachtung lässt auf eine Verbindung zwischen Krebsstammzellen und ID-1 in der Zelllinie P-STS schließen, welche zuvor noch nie erforscht wurde.

Zielsetzung und Strategie: Ziel dieser Arbeit war es, die Auswirkung von ID-1 nach Ausschaltung bzw. Überangebot auf die Charakteristika von Krebsstammzellen in der Zelllinie P-STS zu untersuchen.

Material und Methoden: Mittels lentiviraler Transduktion spezifischer Konstrukte wurde die Expression von ID-1 in P-STS Zellen inhibiert bzw. verstärkt. Die erfolgreiche Expressionsmanipulation wurde auf mRNA- und Proteinebene verifiziert. Basierend auf Überexpression und Inhibierung von ID-1 wurden CSC assoziierte Charakteristika untersucht. Messungen hinsichtlich des Zellwachstums, der Vitalität/Apoptose sowie der Fähigkeit der Tumorformation *in vitro* und *in vivo* wurden durchgeführt.

Ergebnisse: Die Transduktion der P-STS Zellline war erfolgreich. Die Funktionalität der Konstrukte (ID-1 Überexpression bzw. Inhibierung) konnte mittels Analyse der ID-1 Expression nachgewiesen werden. Während die Überexpression von ID-1 Apoptose verminderte, blieben Proliferation und Vitalität unbeeinflusst. Anhand von *in vivo* Assays konnte gezeigt werden, dass die Inhibierung von ID-1 die Fähigkeit der Zelllinie zur Tumorbildung negativ beeinflusst.

Schlussfolgerung: Die Resultate dieser Arbeit deuten darauf hin, dass ID-1 nicht der Hauptregulator von CSC Charakteristika in der P-STS Zelllinie ist, obwohl die Manipulation von ID-1 leichte Veränderungen dieser Charakteristika hervorruft. Die während dieser Arbeit entstandenen transduzierten P-STS Zelllinien werden in Zukunft von enormen Nutzen sein, um die Funktion von ID-1 in der komplexen wenig erforschten Pathophysiologie von gastroentero-pankreatischen neuroendokrinen Tumoren zu untersuchen.

Abstract

Introduction: ID-1 is the first of four discovered members of the inhibition of DNA binding protein family (ID). It consists of a helix-loop-helix motif (HLH) but lacks the ability to directly bind DNA and instead interacts with basic helix-loop-helix (bHLH) transcription factors. ID-1 was shown to be dysregulated in over 20 types of cancer including medullary thyroid carcinoma, a neuroendocrine tumor (NET) of the thyroid gland. Moreover, ID-1 is described as a stem cell marker in normal and malignant tissues. Previous studies in our group revealed the presence of cancer stem cells (CSC) and the expression of ID-1 in the gastroenteropancreatic (GEP) NET cell line P-STS. In addition, ID-1 is upregulated fivefold when P-STS cells grow three dimensionally, suggesting a role in "stem-cell-ness" of P-STS cells.

Aim and strategy: The aim of this work was to discover if ID-1 has an impact on the "stem-cell-ness" characteristics of the P-STS cells. The common loss-of-function and gain-of-function approach was applied and the resulting manipulated P-STS cell lines were further examined for changes in CSC related processes**.**

Methods: ID-1 loss/gain-of-function in the P-STS cell line was achieved by lentiviral transduction. Subsequently, ID-1 mRNA and protein levels within the transduced cells were quantified. The resulting cell lines were examined to get insights into the role of ID-1 in cellular processes like proliferation, viability and cell death. The impact of ID-1 on tumorigenesis was determined by *in vitro* tumor spheroid formation and *in vivo* tumor formation on the chicken chorioallantoic membrane.

Results: The setup of a protocol to manipulate ID-1 expression in the P-STS cell line was successful. Cell proliferation and viability of the P-STS cells were shown to be independent of overexpressed ID-1, whereas the overexpression had slight impact on apoptosis. Dense and plane tumor formation was observed from the ID-1 overexpressing sample and the controls. In contrast, silencing ID-1 lead to plane tumor formation *in vivo*.

Conclusion: Examinations of transduced P-STS cells pointed out that ID-1 alone has slight impacts on CSC characteristics. Therefore, ID-1 is maybe not the main regulator of cancer "stem-cell-ness" in the P-STS cell line. The outcome of this work, however, represents excellent tools to study the function of ID-1 in the poorly understood pathophysiology of gastroenteropancreatic neuroendocrine tumors.

1 Introduction

1.1 Neuroendocrine tumors

Neuroendocrine tumors (NETs) are rare tumors, which develop either sporadic or in a familiar context. They originate from the hormone-producing tissue of the diffuse neuroendocrine system and hence they occur over the whole body including lung, gastrointestinal tract, pancreas and thyroid (Figure 1)[1]. NETs exhibit a heterogeneous variety of symptomatic and clinical characteristics dependent on their site of origin and their produced hormones (*e.g.* serotonin, insulin, somatostatin)[2,3,4]. For instance, flushing, diarrhea, asthma and carcinoid heart disease are syndromes caused by gastrointestinal NETs. In contrast, a pancreatic NET leads to diabetes, gallbladder disease, diarrhea and weight loss[2].

The incidence of NETs has increased fivefold over the last three decades, but therapies, such as somatostatin analogues treatment or radiotherapy and chemotherapy, are still insufficient and the total resection of the affected tissue remains the only curative treatment[5,2].

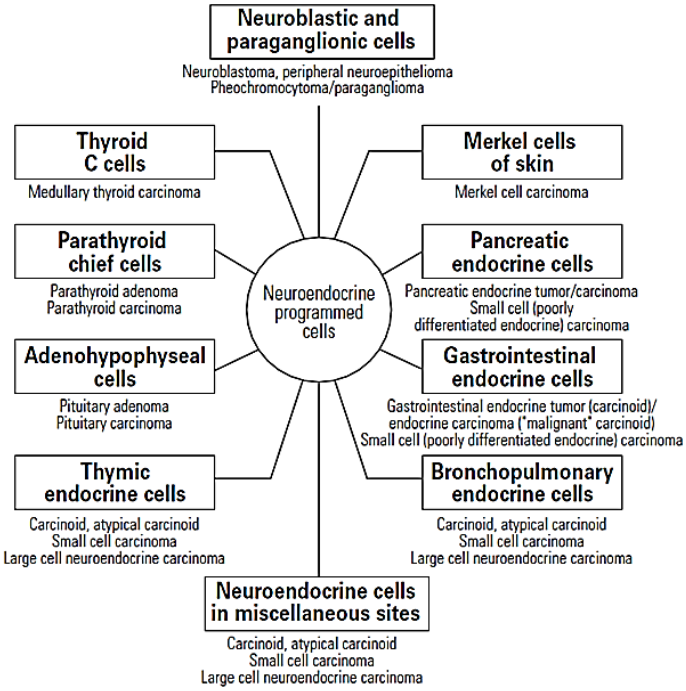

Figure 1: The flowchart gives an overview of the neuroendocrine programmed cells in the human body and the corresponding carcinoma type of the cells[1].

1.1.1. Gastroenteropancreatic neuroendocrine tumors

Gastroenteropancreatic neuroendocrine tumors (GEP-NETs), also known as carcinoids, are multiple, small neoplasms originating from enterochromaffin and enterochromaffin-like cells. They synthesize peptide hormones and bioactive amines (e.g. serotonin, somatostatin, gastrin and histamine)[6], which are either stored in vesicles or secreted mediated by common receptors (*e.g*. G-protein-receptor, ion-

gate receptor)[7]. Most patients have distant metastases at time of diagnosis because the localization of the primary tumor is challenging. Biomarkers such as the glycoprotein chromogranin-A in serum and the vesicle protein synaptophysin in tissue are not as specific as desired and imaging techniques reach their resolution limit due to the small size of the tumor[3].

Little is known about the biology of GEP-NETs, hence there is an urgent need for investigation and understanding the molecular pathophysiology of these tumors.

1.2 Inhibitor of DNA binding protein family

1.2.1 Basic biology and mode of action

Inhibitor of differentiation (ID) proteins are a family of evolutionarily conserved, ubiquitously expressed molecules with important regulatory roles, best studied in *Drosophila melanogaster*. In this organism a single ID-like locus encodes a single ID-like protein[8,9], whereas in human and mice, four ID members (ID-1 – ID-4) have been found, located on different chromosomes (in human: 20q1, 2p25, 1p36 and 6p22-21)[10,11]. ID proteins consist of a helix-loop-helix (HLH) motif, but lack a DNA-binding domain[12]. Each ID protein has at least two isoforms due to alternative splicing sites and the highly conserved N-terminal loop region of the HLH motif is crucial for their activity[13]. ID proteins themselves do not bind to DNA but interact as heterodimers with ubiquitously expressed proteins (E-proteins), like E2A and tissue specific basic HLH (bHLH) transcription factors (TF), such as the ETS protein family. High levels of ID proteins lead to the formation of ID-bHLH/E-protein heterodimers instead of bHLH-bHLH/E-protein or E-protein-E-protein dimers (Figure 2) and hence inhibit binding to the E-Box promoter region. This is a so called negative regulation and causes either a direct inhibition of the DNA binding or the block of a variety of biochemical mechanisms in the cell (*e.g.* Rb and ID-2, chapter 1.2.3)[14,15]. Therefore, ID proteins play an important role in the human embryonic development, but also in several biological processes like cell cycle, senescence as well as tumorigenesis and cancer[12].

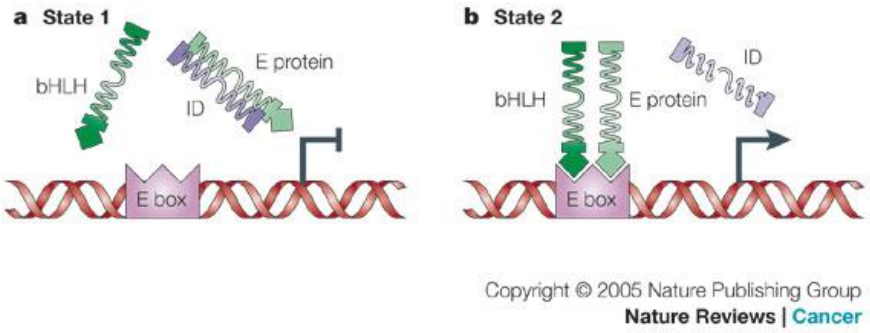

Figure 2: Interaction between ID proteins and bHLH/E-proteins. In state 1 (a), ID proteins form heterodimers with E-proteins (or bHLH, not shown) and inhibit their binding to E-box. When ID proteins are released from the heterodimer (state 2, b) E-proteins form either homodimers (not shown) or heterodimers with bHLH. The dimers then activate transcription[14].

1.2.2 Regulation of ID protein expression

The regulation of ID gene expression is mediated by the members of TGFβ family and is depending on the cell type. In epithelial cells the bone morphogenic protein (BMP) upregulates the expression of ID genes *via* phosphorylation of its downstream signaling proteins Smad1/Smad5. Phosphorylated Smad1/Smad5 then binds to the Smad-binding elements (SBEs) in the ID promoter region and activates transcription[16–19]. In contrast, the transforming growth factor β (TGFβ), represses ID expression *via* phosphorylation of Smad2/Smad3 in epithelial cells. This time binding to the SBE in the ID promoter region ends up in repressing ID transcription[20]. For this, the presence of activating of transcription factor 3 (ATF3) is obligatory. As ATF3 synthesis is induced by TGFβ (and not BMP) Smad3 (and not Smad1) interacts with ATF3 and enables cells to distinguish between TGFβ and BMP signals (Figure 3)[20].

In endothelial cells the biological effect of TGFβ depends on its concentration: in low concentrations, TGFβ upregulates the ID transcription similar to BMP in epithelial cells, whereas high levels of TGFβ suppress ID expression *via* Smad2/Smad3. This is a result of the balance between the activation of the TGFβ receptors Alk1 and Alk5. In presence of high TGFβ levels, Alk5 is more activated than Alk1 and *vice versa*. Activation of Alk5 leads to the expression of the plasminogen activator inhibitor (PAI) *via* Smad2/Smad3. PAI then represses migration and proliferation apparently due to suppressing ID-1[21].

In immune cells, such as dendritic cells, low concentrations of TGFβ induces the expression of ID-2 directly *via* Alk1 and Smad1/Smad5 signaling[22].

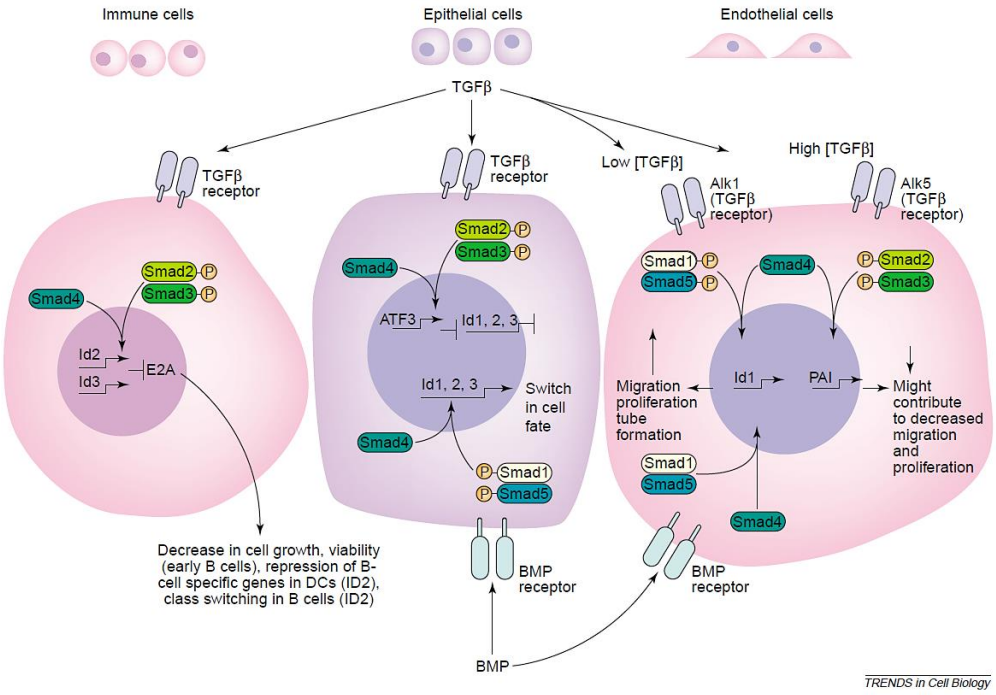

Figure 3: The regulation of ID genes is driven by members of the TGFβ family[12]. BMP is the main signal molecule to enhance ID protein expression, whereas TGFβ counteracts. Both molecules use intracellular Smad signaling to repress/activate the expression ID proteins *via* activating/repressing the promoter of ID proteins. In endothelial cells, TGFβ acts either as activator (Alk1) or inhibitor (Alk5) in combination with the plasminogen activator inhibitor (PAI).

1.2.3 ID proteins in cell cycle and senescence

Besides the inhibitory function of ID proteins, they also play an important role as positive regulators of the cell cycle. The connection between ID proteins and cell cycle is given through the ID mediated repression of p16 and p21, which are cyclin-dependent kinase inhibitors, hence mediators for senescence[12,15,23,24].

During early G1 phase of the cell cycle, mitogenic signals stimulate E26 transformation-specific transcription factors (ETS-TF) to activate the expression of immediate early genes such as c-fos and egr-1[15]. The early growth response protein 1 (EGR-1) activates the expression of ID-1 and ID-3, which inhibit ETS proteins, like ETS1/ETS2 and ETS-TCF ending up with immediate early gene suppression[24]. In turn, ID-1 and ID-3 activate the EGR-1 expression. Inhibition of ETS proteins leads to repression of p16. Therefore, the cyclin-dependent kinases 4 and 6 (CDK 4/6) are able to phosphorylate retinoblastoma proteins (Rb). The phosphorylated Rb proteins release bound ID-2 as well as the transcription factor E2F. The E-protein TF E2A (also known as TCF) is then inhibited by the released ID-2 as well as from EGR-1 mediated expressed ID-1 and ID-3 (Figure 4)[12,25,26].

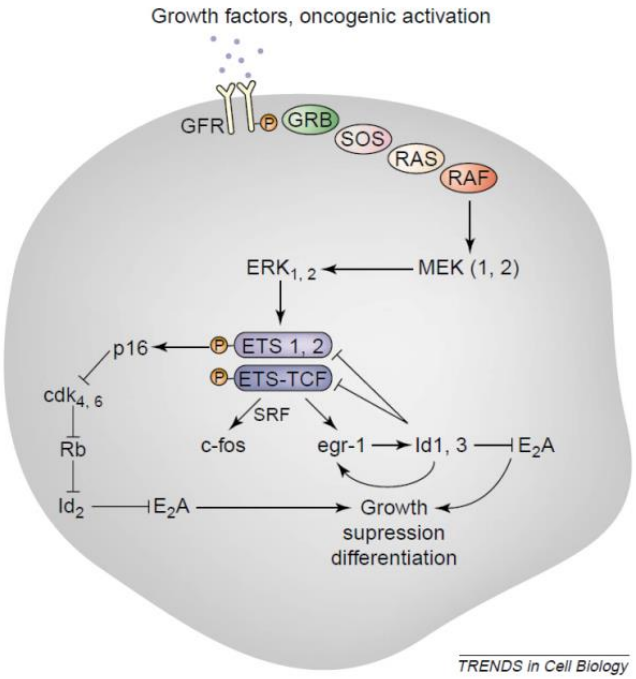

Figure 4: Expression of ID proteins leads to the inhibition of E2A. The mitogenic signals stimulate ETS domain proteins. These proteins activate the expression of ID proteins *via* EGR-1. Besides the repression of ETS proteins, ID proteins regulate EGR-1 expression. The repression of the upstream ETS proteins inactivates p16, which ends up in releasing ID-2 of an Rb-ID-2 complex. All pathways inhibit the E2A transcription factor, which has an important role in different processes of the cell. (Signal cascade of p21 and E2F not shown)[12].

1.2.4 ID proteins associated with cancer

The involvement of ID proteins in cell cycle regulation and senescence gives them a high potential to impact tumorigenesis and cancer when dysregulated. ID proteins are upregulated in several cancer types, such as prostate, breast, colon, rectum, pancreas, liver, leukemia and medullary thyroid carcinoma[27], but ID proteins do not serve as classical oncoproteins[14]. The upregulation is mediated by major oncoproteins, like RAS[28] and MYC[29]. The RAS mediated and mutated p53 driven expression of EGR1 induces the expression of ID-1 and ID-3 (Figure 4)[30,31]. Then ID-1 and ID-3 inhibit the transcription factor ETS1, which, in turn, inhibits p16/p21 and allows the cyclin dependent kinase 4/6 (CDK4/6) to phosphorylate the Rb-ID-2 complex. This restrains more ID-2, which leads to a higher proliferation of cells through the inhibition of E-proteins (*e.g.* E2A/E2F)[14].

In many cancers, ID proteins act as cancer stem cell markers and control the invasiveness of tumor cells *via* progression associated proteins, like the matrix metalloprotease 2 (MMP2), which is highly connected with angiogenesis, cell migration and invasion[32,33].

In mammary epithelial cells, for instance, loss of ID-1 reduces tumor progression, whereas, gain of ID-1 renders noninvasive breast cancer cells invasive[34] and it has been shown that ID-1 plays an important role in the metastatic signature of human breast cancer[35].

1.2.5 ID-1 as cancer stem cell marker

Cancer stem cells (CSCs) represent a small subpopulation of cells in the bulk of tumor cells, which have the ability to drive tumor growth, longtime self-renewing and are claimed to be responsible for resistance to chemotherapy[36]. It has been shown that ID-1 and other ID proteins have a crucial impact on the development of embryonic and adult somatic stem cells in different types of tissue[37]. In colon cancer, as well as in malignant glioma, the function of ID proteins as cancer stem cell marker is best explored[38]. The simultaneous expression of ID-1 and ID-3 in colon CSCs increases the self-renewal capacity and tumor initiation. Silencing both, ID-1 and ID-3, leads to higher sensitivity to the chemotherapeutic oxaliplatin[39]. So far, ID proteins are not well investigated in NETs. By immunohistochemical staining of patient derived specimen, Kebebew *et al.* found ID-1 to be overexpressed in medullary thyroid carcinoma (MTC), a neuroendocrine tumor of the thyroid gland. Moreover, the expression of ID-1 was detected in the MTC cell line TT using Northern blot analysis[27].

Little is known about CSCs in GEP-NETs. The presence of CSCs in patient derived tissue of seven primary tumors as well as in metastasis of carcinoids was found by Gaur *et al.*[40], however, expression of ID proteins in GEP-NET CSCs has not been investigated yet.

1.3 Aims of this work

In our research group, we preliminary found the presence of a small population of cancer stem cells and the expression of ID-1 in the GEP-NET cell line P-STS. Cultivating P-STS cells in *in vitro* tumor spheroids led to a fivefold upregulation of the ID-1 expression. In addition, P-STS tumor spheroids grafted on the chicken chorioallantoic membrane grow with more invasive behavior compared to single cell suspension of the P-STS cell line[41]. Our findings refer ID-1 as a potential cancer stem cell marker in the P-STS cell line.

Based on these data, we hypothesize that ID-1 is a key molecule in “stem-cell-ness” of GEP-NET cell line P-STS. This leads to the aim of my work:

Does ID-1 have an impact on the “stem-cell-ness” characteristics of the P-STS?

To clarify the aim, we chose the common loss-of-function and gain-of-function approach, which lead us to additional, specific aims:

Specific aim #1: Is it possible to downregulate/upregulate ID-1 in the P-STS cell line cell line?

Specific aim #2: What is the impact of ID-1 manipulated P-STS cells on CSC related processes in this cell line?

1.3.1 Workflow of the experimental setup

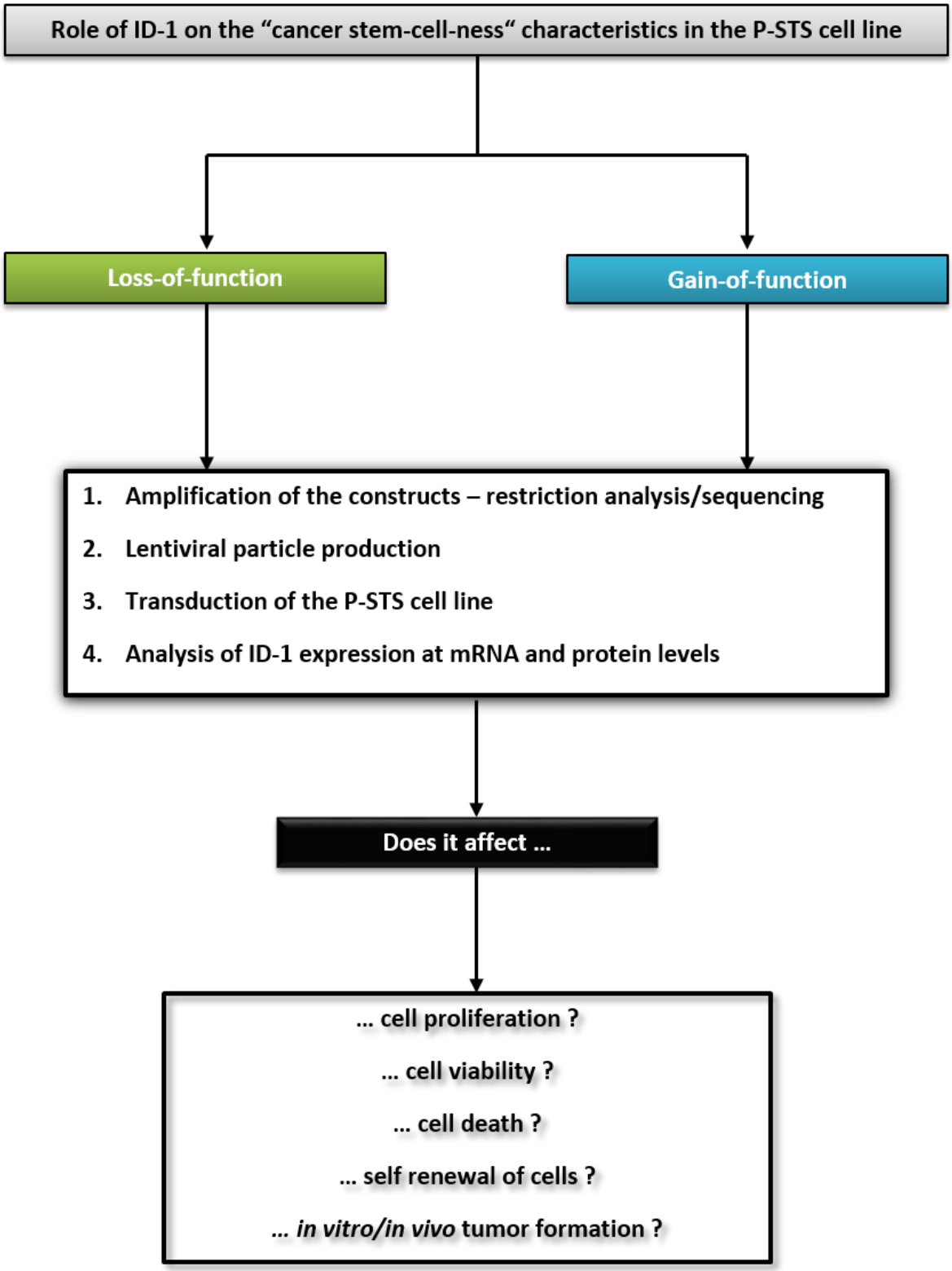

2 Materials and Methods

2.1 Cell lines

2.1.1 Small intestine neuroendocrine tumor cell line P-STS

The P-STS cell line was established from the primary tumor of a small intestine metastatic human carcinoid of a 42-year-old male by Roswitha Pfragner (Medical University of Graz)[42]. The cell line was maintained at 37°C and 5% CO_2, cultured in M199 (Sigma Aldrich, St. Louis) mixed 1:1 with Ham´s F12 (Lonza, Basel) supplemented with 10% FBS (Biochrom, Berlin) and 1% P/S (Sigma Aldrich, St. Louis). Once a week the cell number was adjusted to $2x10^5$ cells/mL by passaging using accutase (Sigma Aldrich, St. Louis). Three days later the cells were fed with the equal volume of medium as on the splitting day.

2.1.2 Human embryonic kidney cell line HEK 293T

HEK 293T cell line is derived from human embryonic kidney tissue purchased from ATCC, which is highly transfectable and therefore widely used for lentiviral particle production. The cell line was maintained at 37°C and 5% CO_2, cultured according to ATCC in DMEM (ATCC, Manassas) supplemented with 10% FBS and 1% P/S.

2.2 Transfection and transduction of the P-STS cell line

2.2.1 Constructs

All constructs were purchased from abm (Canada, Richmond). As general features the constructs express GFP and carry kanamycin resistance as well as the Pac (puromycin *N*-acetyltransferase) gene. The complete vector maps are illustrated in the Appendix 7.2.

2.2.1.1 Lentiviral vectors for ID-1 overexpression – Gain-of-function

To overexpress ID-1, the vector pLenti-GIII-CMV-GFP-2A-Puro backbone (8 829 bp; Figure 5) encoding the sequence of ID-1 (Table 1) was used. The empty backbone vector (BB) served as control. The constructs express GFP under the SV40 promoter and ID-1 expression is driven by CMV promoter.

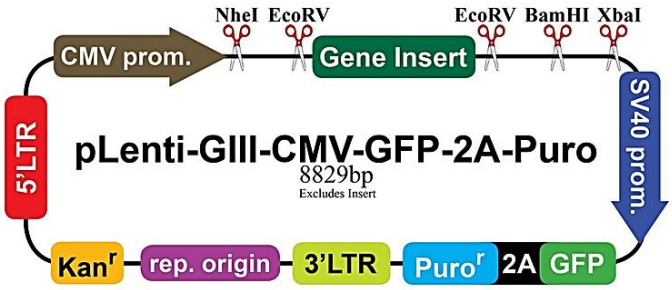

Figure 5: Schematic overview of the construct expressing ID-1.

Table 1: DNA sequence of ID-1 insert of the pLenti-GIII-CMV-GFP-2A-Puro construct.

Gene	Sequence
ID-1	5´-ATGAAAGTCGCCAGTGGCAGCACCGCCACCGCCGCCGCGGGCCCCAGCTGCGCGCTGAAGGCCG GCAAGACAGCGAGCGGTGCGGGCGAGGTGGTGCGCTGTCTGTCTGAGCAGAGCGTGGCCATCTCGC GCTGCGCCGGGGGCGCCGGGGCGCGCCTGCCTGCCCTGCTGGACGAGCAGCAGGTAAACGTGCTGC TCTACGACATGAACGGCTGTTACTCACGCCTCAAGGAGCTGGTGCCCACCCTGCCCCAGAACCGCAAG GTGAGCAAGGTGGAGATTCTCCAGCACGTCATCGACTACATCAGGGACCTTCAGTTGGAGCTGAACTC GGAATCCGAAGTTGGAACCCCCGGGGGCCGAGGGCTGCCGGTCCGGGCTCCGCTCAGCACCCTCAAC GGCGAGATCAGCGCCCTGACGGCCGAGGCGGCATGCGTTCCTGCGGACGATCGCATCTTGTGTCGCT GCCCAACTTTCTTGTACAAAGTGGTTGATATCTGA-3´

2.2.1.2 Lentiviral vectors for silencing ID-1 – Loss-of-function

For the silencing of ID-1 in the P-STS cell line, two different siRNAs and a scrambled control (scr) plasmid were used. The target sequences of the siRNAs (siA and siB) are listed in Table 2. The lentiviral plasmid piLenti-siRNA-GFP (9 043 bp) containing a GFP gene under the control of the CMV promoter serves as backbone. Each small interfering RNA is expressed under the U6 promoter (Figure 6).

Table 2: ID-1 targeting siRNA sequences of the constructs.

Construct	Targeting sequence
scrambled control (scr)[43]	5'-GGGTGAACTCACGTCAGAA-3´
siRNA variant A (siA)	5´-CGACATGAACGGCTGTTACTCACGCCTCA-3´
siRNA variant B (siB)	5´-AAGGTGAGCAAGGTGGAGATT-3´

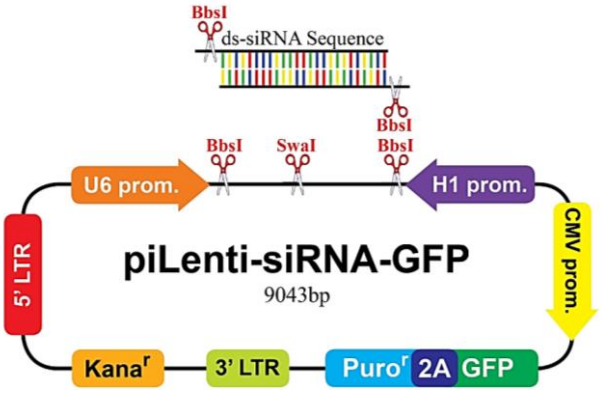

Figure 6: Schematic overview of the construct silencing ID-1.

2.3 Transformation, plasmid isolation and purification

2.3.1 Heat-Shock transformation of competent *Escherichia coli*

The chemical competent *E. coli* strain DH5α™ (Library Efficiency©, Invitrogen, Carlsbad) was used to amplify plasmid DNA. The competent cells were thawed on ice and 100 µL were incubated for 30 min with 10 ng plasmid DNA. Heat-shock transformation took place at 42°C for 45 sec. Then S.O.C medium was added and the cells were allowed to recover for 1 h at 37°C, shaked with 225 rpm. Bacterial suspension (10, 20, 50, 100, 200 µL each) was plated on LB-agar plates containing 50 µg/mL kanamycin. On the next day single colony picking was performed to inoculate shaking flasks containing 3 mL LB-medium (50 µg/mL kanamycin). After 8 h, 50 µL of the culture were taken to inoculate 25 mL LB-medium (50 µg/mL kanamycin). For the right cell density, this culture was incubated overnight with 225 rpm at 37°C.

2.3.2 Plasmid isolation and purification

To isolate and purify the plasmids a midiprep (Qiagen, Venlo) was performed according to the plasmid purification handbook. In short, the cells were harvested *via* centrifugation (6 000 x g) for 15 min at 4°C. The pellet was resuspended and alkaline lysis buffer was added. For the precipitation of proteins, genomic DNA and cell debris, acidic pre-chilled buffer was added. To get rid of all the precipitated material a centrifugation step (20 000 x g) was performed at 4°C for 30 min. The supernatant containing the plasmid was centrifuged at 20 000 x g again. To purify the plasmid a pre-equilibrated column was used. The supernatant was loaded on the column, followed by two washing steps and the elution with water. The fraction was mixed with isopropanol and centrifuged at 15 000 x g for 30 min at 4°C. Then the pellet containing the plasmid DNA was washed with 70% ethanol and centrifuged at 15 000 x g for 10 min. The supernatant was decanted and the received pellet was redissolved in water. The plasmid DNA concentration was measured with Nanodrop© (ND-1000; peqlab, Erlangen).

2.3.3 Analysis of the plasmid

To check if the correct plasmid was isolated, 500 ng/µL plasmid DNA was digested with FastDigest© *Hind*III (Thermo Scientific, Waltham) for 5 min at 37°C, followed by gel electrophoresis (1.5%, 70 V for 70 min) and ethidium bromide staining. Simultaneously, an *in silico* digestion using ApE plasmid editor (Copyright by M. Wayne Davis; http://biologylabs.utah.edu/jorgensen/wayned/ape/) was done.

To ensure that the plasmids are intact and no mutations took place during the amplification, 1 000 ng of each plasmid were sent for sequencing to the company Microsynth (Austria, Vienna). Forward sequencing was performed with primers for the U6 promoter to sequence the plasmids for the

silencing experiment and primers for CMV promoter were used for sequencing the overexpression and control plasmids.

2.4 Lentivirus packaging

The production of lentiviral particles was performed according to the manufacturers protocol using HEK 293T (p16) cells. If not mentioned else, all substances for this experiment were purchased from abm (Canada, Richmond). All steps were performed under safety level 2 conditions. A negative (no plasmid) control was included for each sample.

On day 1 of the experiment $2x10^6$ cells were seeded in a 10 cm tissue culture dish. After checking the confluency (70-80%) on the next day, following solutions were prepared:

Solution 1:

10 µg plasmid and 10 µg abm´s 3rd generation packaging mix in 1 mL serum free, antibiotic free medium.

Solution 2:

80 µL of LentiFectin™ in 1 mL serum free, antibiotic free medium.

Both solutions were incubated at room temperature for 5 min and then mixed together and incubated for another 20 min to create the transfection complex. After the incubation 4.5 mL of serum free, antibiotic free medium was added to the complex.

The medium of the cells was removed and the transfection complex was added gently drop by drop on the cells without detaching them. The cells were then incubated for 8 h at 37°C and 5% CO_2. After the incubation 650 µL FBS were added and the cells were incubated again over night.

On the third day, the transfection complex medium was removed and 10 mL of complete medium were added gently to the cells. For the production of the viral particles the cells were incubated 24 h, the supernatant was harvested and fresh medium was added. The supernatant was centrifuged at 3 000 x g and 4°C to get rid of cell debris. The cleared supernatant was filtered with a low protein-binding 0.45 µm sterile filter. On the next day, a second harvest was done as described previously. The second harvest was then added to the first and stored at 4°C.

2.5 Lentiviral transduction of P-STS cells

To transduce the P-STS cell line $5x10^5$ cells were seeded in a 6-well tissue culture plate and incubated over night at 37°C and 5% CO_2 allowing them to attach. On the next day, the transduction was performed using 0.75 mL virus supernatant, 0.5 mL complete media supplemented with 0.2 µL (2 µg)

of a 10 µg/µL polybrene solution (Santa Cruz Biotechnology, Dallas). The medium was removed and the transduction mix was added to the cells. After 24 and 48 hours of incubation the transduction was repeated as described before. After the third incubation all P-STS cells were harvested and cultured under normal culture conditions until they became confluent.

2.6 Quantification of transfection efficiency

2.6.1 FACS analysis of GFP^+ population and cell sorting

To test the percentage of GFP^+ cells in the population, cells were harvested using accutase. $1x10^6$ cells were washed twice, resuspended in 500 µL pre-warmed CMF-PBS and analyzed with BD FACSAriaII™ at the flow cytometry core facility of the Medical University of Graz. Simultaneously, single GFP^+ cells were sorted.

2.6.2 Selection of transfected cells and flow cytometry analysis of GFP^+ population

To enrich the positive transfected cells, the culture medium was supplemented with 2 µg/mL puromycin. After three days of incubation the medium was refreshed with normal culture medium until the cells became confluent. To measure the amount of GFP^+ cells in the puromycin treated population flow cytometry analysis (BD LSR Fortessa™) was done as described previously (chapter 2.6.1).

2.7 Quantification of ID-1 mRNA

2.7.1 RNA isolation

To isolate RNA of the cells, $2x10^6$ cells were lysed in TriReagentRT (Molecular research center, Cincinnati). After the homogenization 50 µL 4-bromoanisole (BAN) were added and mixed properly. Then the solution was incubated for 5 min and centrifuged at 12 000 x g for 15 min at 4°C. The aqueous phase was transferred and the RNA was precipitated by adding 500 µL isopropanol. After 10 min incubation at RT the mixture was centrifuged again at 12 000 x g for 8 min at 4°C. The supernatant was removed and a washing step with 1 mL 70% ethanol was done. Then the supernatant was removed carefully without removing the visible pellet. The pellet was air-dried for 5 min and dissolved in an appropriate amount of RNAse free water for 10 min at 55°C and 300 rpm on the heat-block. The RNA concentration was measured by NanoDrop©.

2.7.2 cDNA synthesis

To analyze the expression levels of ID-1 the isolated RNA had to be synthesized to cDNA. Therefore, the enzyme reverse transcriptase was used. Table 3 shows the RT-PCR reaction mix (Applied Biosystems High capacity RNA to cDNA Kit).

Table 3: General reaction mix to synthesize cDNA.

Substance	Volume [µL]
10x RT buffer	2
25x dNTP mix (100 mM)	0.8
10x Random primer	2
RT enzyme	1
H_2O	4.2
In total	**10 µL**

The RNA was diluted to 2 000 pg in 10 µL and the reaction mix was added to the diluted RNA. All reactions included a control (no reverse transcriptase). The temperature program (32 cycles) for the thermocycler (BioRaq C1000 thermocycler) was as following:

Table 4: Thermocycler program for the RT-PCR; 32 cycles were performed using a reaction volume of 20 µL.

Time	Temperature
10 min	25°C
120 min	37°C
5 sec	85°C
Infinity [∞]	4°C

2.7.3 qPCR and expression analysis

For the analysis of RNA expression levels qPCR employing SYBR© Green (Bio-Rad, Vienna) was used. All reactions contained a control of the RT-PCR and a no template control (NTC). First, the cDNA was diluted 1:4 to reach a concentration of 5 ng/µL. To amplify the cDNA of ID-1, the primers (Invitrogen, Carlsbad) according to Locklin *et al.* were used. For the quantification the housekeeping gene β-actin was used.

Table 5: PCR primers of the ID familiy[44] and the housekeeping gene β-actin.

Gene	RefSeq no.	Primer location	Sequence	Product length (bp)
ID-1	NM_002165.3	5´-113	5´-TGGTCGCTGTCTGTCTGAG-3´	300
	NM_181353.2	3´-403	5´-GCCGTTGAGGGTGCTGAG-3´	
ID-2	NM_002166.4	5´-197	5´-ACGACCCGATGAGCCTGCTA-3´	213
		3´-391	5´-TCCTGGAGCGCTGGTTCTG-3´	
ID-3	NM_002167.4	5´-480	5´-TGAGCTTGCTGGACGAC-3´	571
		3´-1031	5´-CCTTGGCATAGTTTGGAGAG-3´	
ID-4	NM_001546.3	5´-230	5´-GTGCGATATGAACGACTGCT-3´	358
		3´-569	5´-TCTTCCCCCTCCCTCTCTA-3´	
β-actin	NM_001101.3	Forward	5´-CATGTACGTTGCTATCCAGGC-3´	250
		Reverse	5´-CTCCTTAATGTCACGCACGAT-3´	

For the reaction mix following volumes and concentrations were used:

Table 6: General reaction mix of the qPCR in 15 µl.

Substance	Volume [µL]
IQ™ SYBR© Green Supermix	7.50
Primer fwd. (0.3 µM)	0.30
Primer rev. (0.3 µM)	0.30
cDNA (5 ng/µL)	4.00
H_2O	2.90
In total	**15 µL**

Following table shows the temperature program (Real-Time CFX96 System, Bio-Rad) for the qPCR reaction, 40 cycles were performed:

Table 7: Temperature program (40 cycles) for the qPCR analysis of ID-1 and β-actin.

Time	Temperature
3 min	95°C
10 sec	95°C
40 sec	60°C
10 sec	55°C

For a better interpretation of the amplificates, a melting curve was done subsequently. Therefore, the temperature was increased from 55°C to 95°C in 0.5°C steps and the relative florescence unit (RFU) was measured every 10 sec. To calculate the levels of ID-1 expression, the ΔΔCq[45,46] method was used.

2.8 Western blot analysis

2.8.1 Protein isolation and BCA assay

For a whole protein isolation 2-5x10^6 cells of all samples were harvested (350 x g, 5 min), washed twice with pre-chilled CMF-PBS and frozen at -20°C. On the next day the pellet was lysed by resuspending it in a proper amount (70-150 µL) of protein lysis buffer, vortexed for 30 sec and sonicated in a pre-chilled water bath sonicator two times for 3 min. After the sonication a centrifugation step was performed at 4°C with 350 x g for 10 min to remove the DNA. The supernatant was transferred into a new tube and the protein concentration was determined *via* BCA[47] assay (Pierce™ BCA Protein assay Kit, Thermo Scientific).

Therefore, 4 µL of the supernatant were added into a 96 well plate. A five-point calibration of BSA (200 mg/mL) was used. The concentrations were 2, 1.5, 1, 0.5 and 0 mg/mL BSA. Then, 100 µL of BCA reagent was added to the protein lysate, incubated for 30 min at 37°C and the absorption at 562 nm

was measured (Sunrise, Tecan). All samples were measured as triplicates and linear regression was used to determine the protein concentration.

2.8.2 SDS – PAGE

For separating the proteins according to their size, SDS-PAGE[48] was used with following compositions of separating and stacking gel:

Table 8: Volumes of used substances for the SDS-PAGE.

Separating gel	**12% SDS - PAGE**
Acrylamide 40%	2.4 mL
1.5 M TRIS pH 8.8	2.0 mL
H_2O	3.4 mL
SDS 10%	80 µl
TEMED	8 µL
APS 10%	8 µL
In total	**8 mL**

Stacking gel	**4% SDS - PAGE**
Acrylamide 40%	0.4 mL
1 M TRIS pH 6.8	1.0 mL
H_2O	2.5 mL
SDS 10%	40 µL
TEMED	4 µL
APS 10%	40 µL
In total	**4 mL**

A total protein amount of 15 µg was mixed with a 4x loading dye (XT sample buffer; Bio-Rad), incubated on a heat block at 95°C for 5 min, and loaded on the gel. 12 µL of the standard (Novex© sharp Pre-Stained) and 2 µL of MagicMark™ (Novex©, Life technologies) were loaded in the same gel pocket. The gel run was performed at 120 V for 90 min.

2.8.3 Blotting

For the semi-dry blotting[49] of the separated proteins, a PVDF membrane was used. In short, the used materials (transfer cassette, sponges, filter papers and gel) were soaked in transfer buffer for 10 min and the membrane was activated in methanol for 15 sec before equilibration. The gadgets were put together in the way that the proteins were blotted in the correct direction.

The set up for the blotting was 100 V for 30 min under cooling of the buffer and constant stirring. After the process, the membrane was washed three times shortly with 0.1% TBS-T buffer and blocked for 3 h with 5% milk powder (Blotting-Grade Blocker; Bio-Rad) in 0.1% TBS-T.

2.8.4 Protein detection

The blocked membrane was incubated with diluted primary antibody (Table 9) in 5% milk powder (0.1% TBS-T) over night at 4°C. On the next day the membrane was washed properly to remove all non-bound primary antibody and incubated 1.5 h at room temperature with secondary antibody diluted in 5% milk powder (0.1% TBS-T). Then the blot was washed with 0.1% TBS-T to remove unbound secondary antibody.

Table 9: Used dilutions of the antibodies for the detection and quantification of ID-1.

Antibody	**Dilution**
Rabbit anti-human ID-1 (Bioss, Woburn)	1:750
Rabbit anti-human β-actin (Sigma Aldrich, St. Louis)	1:5 000
Goat anti-rabbit IgG – HRP (Santa Cruz Biotechnology, Dallas)	1:6 000

For the protein detection the membrane was incubated for 5 min with ECL substrate (Clarity western ECL Substrate, Bio-Rad). Then, an x-ray film (CL-XPosure™ Film, Thermo Scientific) was placed on the membrane in a film cassette. After proper exposure time the film was placed in developer to visualize protein signal. Then the film was washed, fixed and washed again with water and air dried.

To quantify the obtained signal the film was scanned and ImageJ[50] was used to densitometrically calculate the intensities of the bands. For the quantification the signal of the loading control (β-actin) was used.

2.8.5 Immunostaining of the cells

For staining ID-1, the cells were harvested, washed in CMF-PBS and cytospins were performed using flexiPERM™ (Greiner, Kremsmünster). Therefore, the cells were centrifuged at 800 rpm for 10 min, fixed with 4% PFA and washed three times with 0.1% TBS-T.

2.8.5.1 Immunohistochemistry

The Mouse and Rabbit Specific HRP/DAB (ABC) Detection IHC kit (abcam, Cambridge) was used. In short, first, a hydrogen peroxidase block and second, a protein block was applied. Then, the cells were incubated with primary ID-1 antibody (1:750) over night at 4°C. On the next day, the slides were incubated with biotinylated secondary antibody. After several washing steps, streptavidin peroxidase

was added to the slides. The chromogen was diluted 1:50 with the DAB substrate and added to the slides. The reaction was stopped and cells were stained with hematoxylin.

2.8.5.2 Immunofluorescence

For the subcellular localization of ID-1, immunofluorescence staining was performed. After the blocking step, the primary ID-1 antibody (1:750) was incubated over night at 4°C. On the next day, the slides were washed and incubated with secondary antibody for 30 min. Afterwards, a nuclear DAPI staining was done for 20 min.

Table 10: Used antibodies and dilutions for the immunofluorescence staining.

Antibody	**Dilution**
Rabbit anti-human ID-1 (Bioss, Woburn)	1:750 with Antibody Diluent (Dako)
Normal rabbit IgG (Santa Cruz Biotechnology, Dallas)	1:750 with Antibody Diluent (Dako)
CY™3-conjugated AffiniPure goat anti-rabbit IgG (H+L) (Jackson ImmunoResearch Lab, West Grove)	1:800 with Antibody Diluent (Dako)
DAPI Nucleic Acid Stain (Life Technologies, Carlsbad)	1:1 000 with 0.1% TBS-T

2.9 Proliferation, viability and apoptosis and assays

On the first day $2x10^5$ cells/mL were seeded in a 24-well plate. On the next three days, the cells were resuspended consistently to detach them from the surface. This plate was used to perform the following three assays. All experiments were performed at least in triplicates.

2.9.1 Proliferation assay

Proliferation of cells was determined by cell counting based on the integrity of plasma membrane. At different time points, 50 µL cell suspension were mixed with 10 mL CASY-Ton (Roche, Vienna) and measured *via* CASY© TTC Cell Counter & Analyzer (Schärfe System; Roche, Vienna).

2.9.2 Viability assay

The viability of a cell corresponds to its mitochondrial activity, which can be measured after the cleavage of tetrazolium salts (WST-1) to formazan by mitochondrial enzymes[51]. Briefly, 100 µL of detached cells were placed into a 96-well plate, then 10 µL WST-1 reagent/well was added (Roche, Vienna). After 1 h of incubation the absorbance at 450 nm (reference wavelength: 650 nm) was measured (ThermoMax, Molecular devices) and analyzed.

2.9.3 Apoptosis assay

The activity of caspase 3/7 is a direct parameter for cell death status, it is measured by cleaving luminogenic substrate, which then releases a substrate (DEVD) for aminoluciferin[52]. This leads to the

measurable production of light. For this experiment the Caspase-Glo© 3/7 assay (Promega, Madison) was used. Therefore, 50 µL of the detached cells were placed into a white microwell plate and mixed with 50 µL substrate. After 1 h of incubation the luminescence was measured (GlowMax©, Promega) and statistically analyzed.

2.10 Tumor formation

2.10.1 *In vitro* tumor spheroid formation assay

To test the self-renewal capacity of the transduced cells, a tumor spheroid formation assay was performed[53]. For this purpose, the cell suspension was diluted to one single cell in 200 µL. The medium was exchanged to a specific serum free medium containing F12/M199 (1:1) supplemented with 20 ng/mL human EGF (Peprotech, New York), 10 ng/mL human bFGF (Prepotech, New York), 2% B27 Supplement (Gibco; Life technologies, Carlsbad) and 300IU Heparin (Baxter, Vienna). The spheroid formation was observed for 7 days.

2.10.2 *In vivo* chorioallantoic membrane assay

For the information if ID-1 is essential for P-STS to form a dense tumor the chicken chorioallantoic membrane (CAM) was used according to Quigley *et al.*[54]. Fertilized white Leghorn eggs (Schropper, Gloggnitz) were cleaned and wiped with 5% H_2O_2. Afterwards the eggs were incubated for three days at 37.6°C and 70-75% humidity under permanent rotation. After the incubation, the eggs were cleaned with 70% ethanol and cracked carefully. Under slight pressure the eggshell was opened, the albumen and intact yolk were caught in a pre-sterilized, covered dish and incubated stationary at 37.6°C and 70-75% humidity for 7 days.

At day ten of the *ex ovo* embryonic development $1x10^6$ cells were resuspended in 20 µL CMF-PBS and grafted on the CAM. To avoid a leak of the cell suspension 0.5 mm thin silicone rings (Ø 5 mm) were used for border. Afterwards, the chicken embryos were incubated for three further days and the tumor formation was observed macroscopically.

2.11 Statistical analysis of the results

The statistical tests[55] were calculated with GraphPad Prism version 6.00 for Windows (GraphPad Software, La Jolla, www.graphpad.com) and the resulting p values were marked in the graphs.

3 Results

3.1 Expression pattern of ID family members in the P-STS cell line

Messenger RNA of all ID family members, predominantly ID-1 and ID-3, were found in the P-STS cell line using semi-quantitative RT-PCR and subsequent electrophoresis. ID-2 showed the lowest expression (Figure 7).

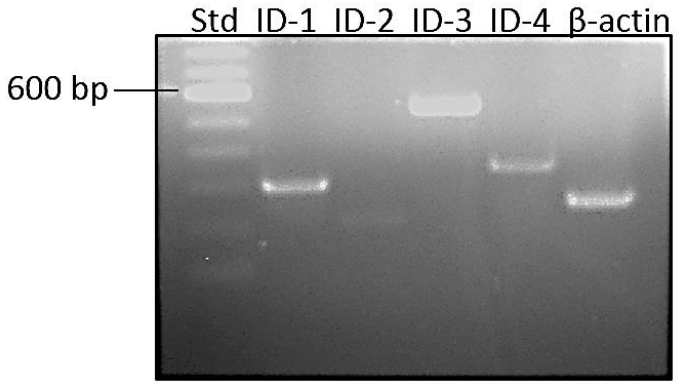

Figure 7: Agarose gel electrophoresis of PCR fragments. All ID protein family members were expressed in the P-STS cell line (100 bp Standard). The house-keeping gene β-actin served as positive control.

3.2 Analysis of the plasmids

3.2.1 Restriction analysis

Prior to restriction analysis, *in silico Hind*III digestion of all lentiviral plasmids used in this work was performed, which revealed five DNA fragments as listed in Table 11. The same result was found after digestion of the plasmids with *Hind*III (Figure 8). In two samples (ID-1 and siA) undigested and partial digested fragments were found because of uncompleted digestion (Figure 8 -Arrows).

Table 11: Fragments (bp) of the *in silico* digestion of all plasmids using ApE plasmid editor.

	Fragments [bp]				
	BB	**ID-1**	**scr**	**siA**	**siB**
	4 089	4 089	4 089	4 089	4 089
	3 465	3 766	3 441	3 451	3 443
	581	581	581	581	581
	556	556	556	556	556
	352	352	352	352	352
∑	**9 043**	**9 344**	**9 019**	**9 029**	**9 021**

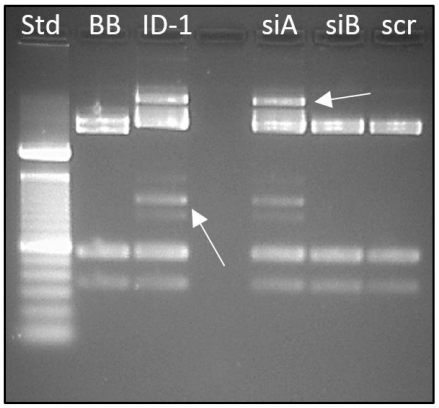

Figure 8: Agarose gel of *Hind*III digestion of the plasmid DNA (100 bp standard). Arrows show undigested fragments.

3.2.2 Sequencing analysis

The results of the sequencing from the company Microsynth (Austria, Vienna) and subsequent alignment[56] showed that all five constructs have the same sequence base pairs (identity) as known from the company (abm), hence no mutation happened during amplification of the plasmids. All chromatograms and plasmid maps are listed in the Appendix 7.3.

Table 12: Results of the sequence alignments of all constructs. All of them are 100% identic to the obtained sequence.

Construct	Identity [%]
BB	100
ID-1	100
scr	100
siA	100
siB	100

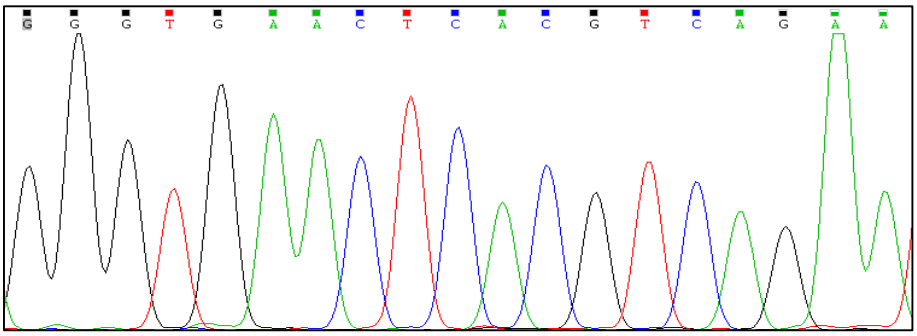

Figure 9: Representative electropherogram of the scr construct.

3.3 Transfection of HEK 293T cells

The transfection of HEK 293T cells according to the manufacturers protocol resulted in GFP expressing HEK 293T cells after the second round of transfection. The negative control remained GFP negative (data not shown).

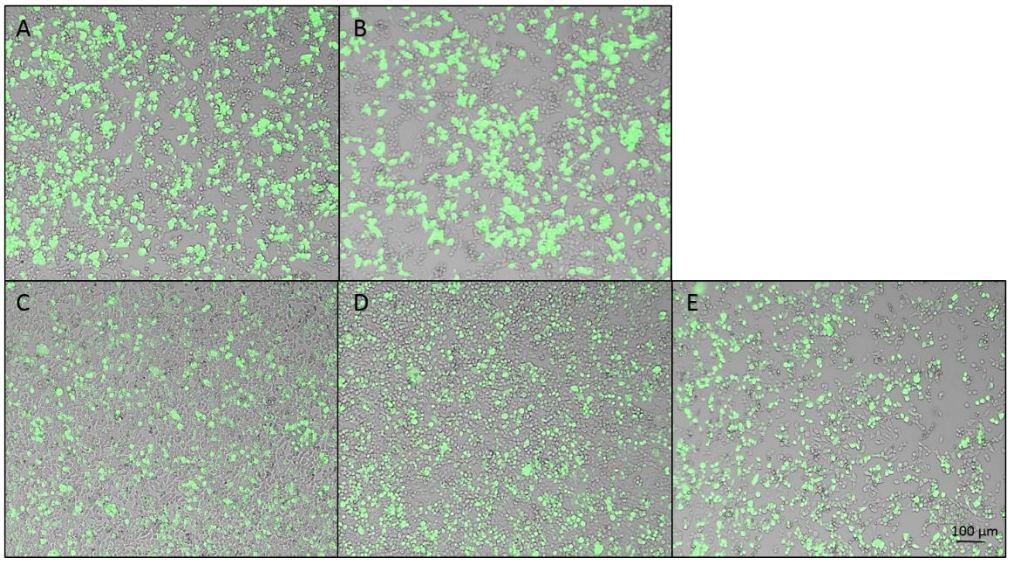

Figure 10: HEK 293T cells were GFP positive after the second transfection. A= BB, B= ID-1, C= scr, D= siA and E= siB; Bar= 100 µm. All pictures were merged (Interphase and fluorescence).

3.4 Transduction of the P-STS cell line and FACS analysis

After three rounds of treatment with the lentiviral particle containing supernatant of the HEK 293T cells, the P-STS cells expressed GFP (Figure 11-Arrows).

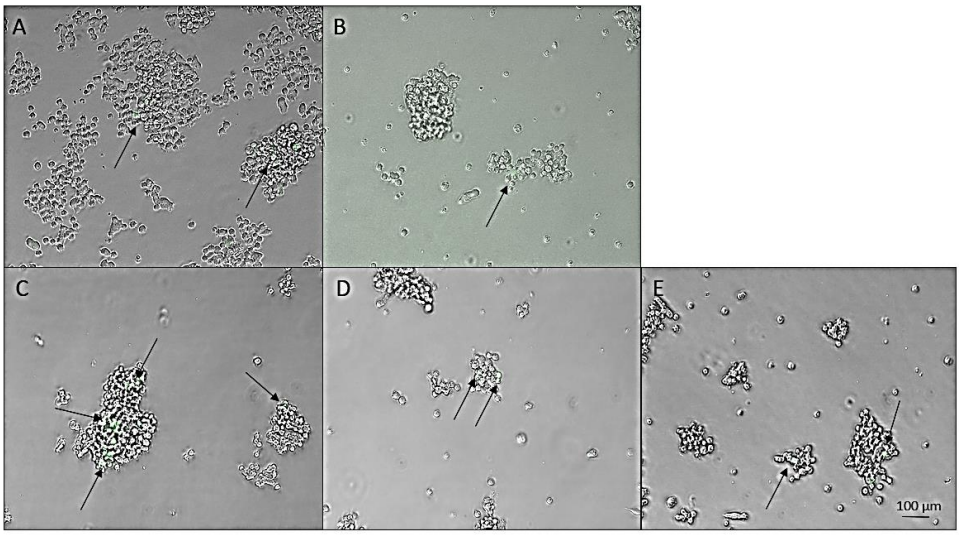

Figure 11: P-STS cells expressed GFP after transduction. Arrows mark the GFP positive cells. A= BB, B= ID-1, C= scr, D= siA, E= siB; Bar= 100 µm. All pictures were merged (Interphase and fluorescence).

The efficiency of the transduction was measured *via* the amount of GFP positive cells in the whole population. This was done using FACS analysis (FacsAriaII™) at the center of biomedical research (Medical University of Graz). Single cells were sorted out of the population to get rid of all non-transduced cells. Table 13 shows the percentage of GFP^+ cells, hence efficiency, and the counts of the sorting. The overall outcome from FACS measurements is enclosed in the Appendix 7.4.

Table 13: Efficiency analysis of the transduced P-STS cells with according counts for single cell sorting.

Sample	GFP^+ population [%]	Counts
BB	0.7	1 700
ID-1	0.1	106
scr	1.5	4 900
siA	0.7	2 100
siB	2.0	1 130

Additionally, cells were treated with 2 µg/mL puromycin to enrich the amount of positively transduced cells. This led to following percentage of GFP positive cells in the population (BD FACSFortessa™).

Table 14: Percentage of GFP positive P-STS cells after treatment with 2 µg/mL puromycin.

Sample	GFP^+ population [%]
BB	83.9
ID-1	68.1
scr	96.2
siA	95.8
siB	96.9

The subsequent experiments were performed with the puromycin selected cells. The FACS sorted samples were frozen (full media supplemented with 10% DMSO) and stored in liquid nitrogen.

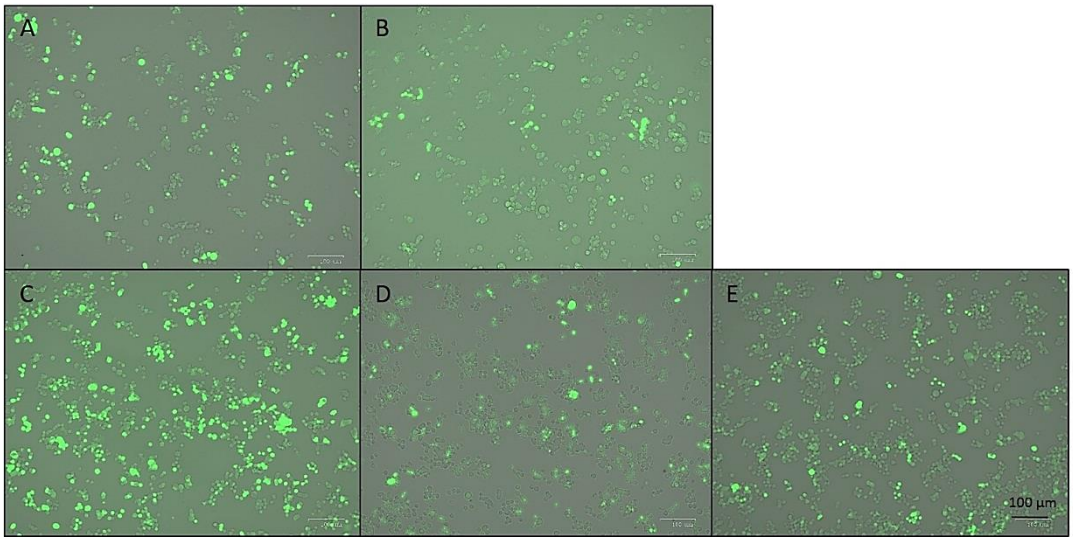

Figure 12: Treatment of transduced P-STS with puromycin (2 µg/mL) enriched the amount of positively transduced cells. A= BB, B= ID-1, C= scr, D= siA, E= siB; Bar= 100 µm. All pictures were merged (Interphase and fluorescence).

The ID-1 overexpressing sample had a smaller GFP^+ cell population. Compared to the other samples (Table 14) the cells, however, were viable and puromycin resistant. The wild type cells (WT) still remained GFP negative and died after puromycin treatment (data not shown).

3.5 Expression analysis of ID-1 in the P-STS cells after transduction

3.5.1 mRNA level

A qPCR was performed to identify the alteration of ID-1 mRNA expression after transduction with lentiviral plasmids. The housekeeping gene β-actin served as control gene, which should not be affected by transduction. The expression was normalized to the corresponding control. To make sure that the control plasmids did not affect the expression, a control group analysis was done (Figure 13-A). The ID-1 mRNA was significantly downregulated threefold in P-STS cells transduced with both siA (twentyfold) and siB (fivefold) constructs (Figure 13-B). ID-1 overexpression was found in P-STS cells transduced with ID-1 construct at mRNA level (fourfold) (Figure 13-C). The level of ID1 mRNA was also altered in P-STS cells transduced with empty vectors (Figure 13-A).

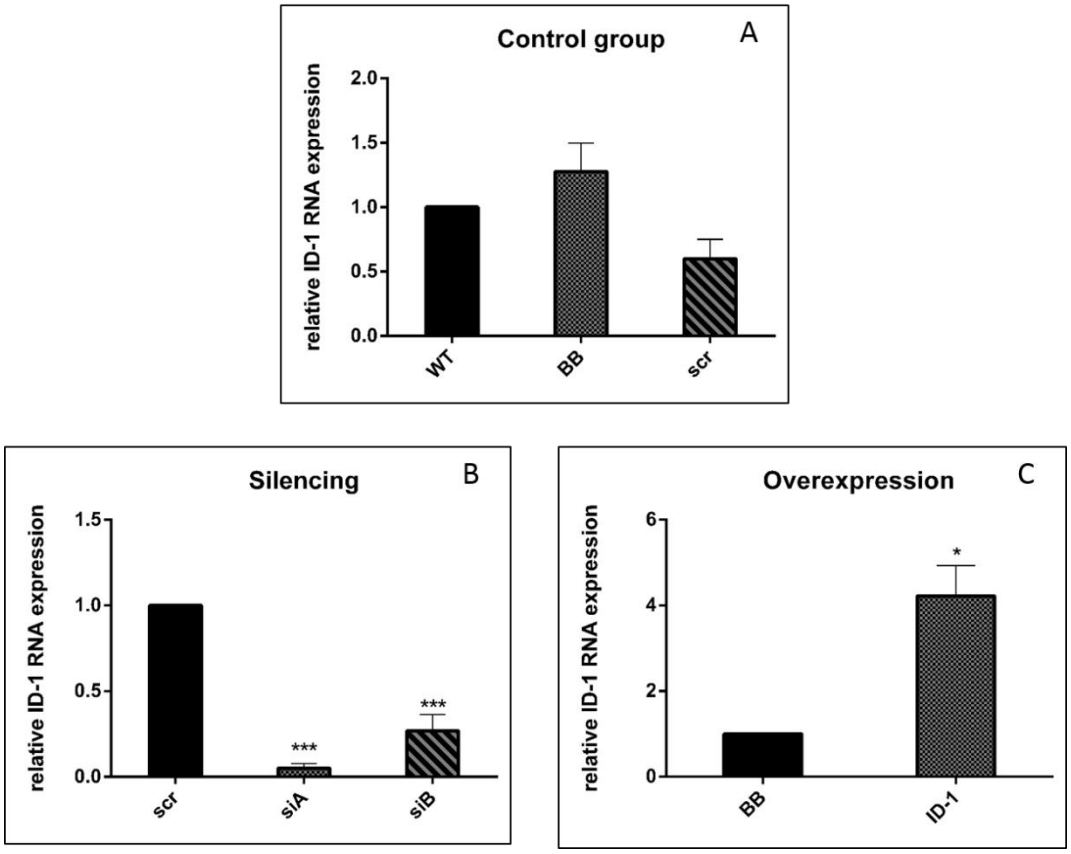

Figure 13: Expression analysis of ID-1 RNA levels with qPCR showed the decrease/increase of ID-1 after transduction. The graphs represent the mean and the SEM of the measurements (n=3). A= Control group, B= loss-of-function experiment, C= gain-of-function experiment. WT = Wild type.

3.5.2 Protein level

3.5.2.1 Western blot analysis

The Western blot analysis was done using 15 µg protein, ID-1 antibody (1:750) and β-actin antibody (1:5 000). P-STS cells transduced with siA and siB constructs had reduced ID-1 protein amount according to their controls (fivefold and 16-fold, respectively, Figure 14). Additionally, Figure 14–B shows the two different isoforms of ID-1 and somehow, the silencing affected one isoform (a) more than the other (b). The overexpression of ID-1 was not detectable *via* Western blot.

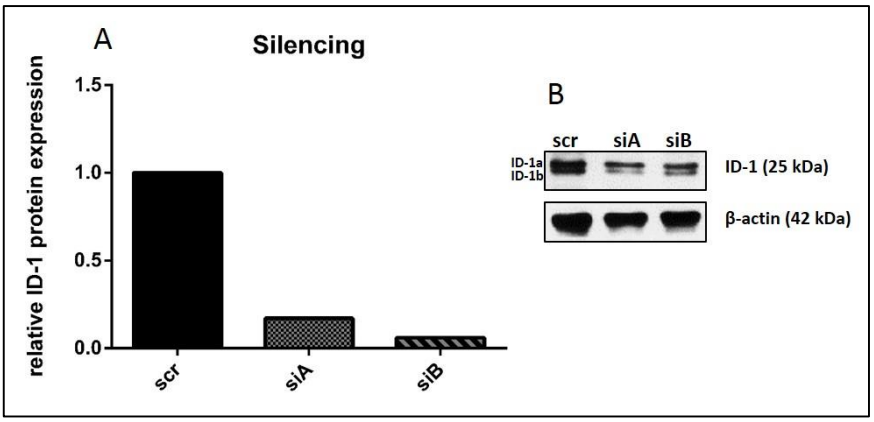

Figure 14: Western blot analysis of the silenced P-STS cells normalized to β-actin (n=1). Both silenced cells had a lower ID-1 protein level than the control. A= quantification data B= representative Western blots of ID-1 and ß-actin.

3.5.2.2 Immunohistochemistry

Immunohistochemistry was performed to show the subcellular localization of ID-1 in P-STS cells. ID-1 protein could be detected in WT cells as well as in cells transduced with all constructs used in this work (Figure 15-Arrows). Rabbit IgG served as negative control (Figure 16). In the P-STS cells ID-1 is localized predominantly in the cytoplasm than in the nucleus.

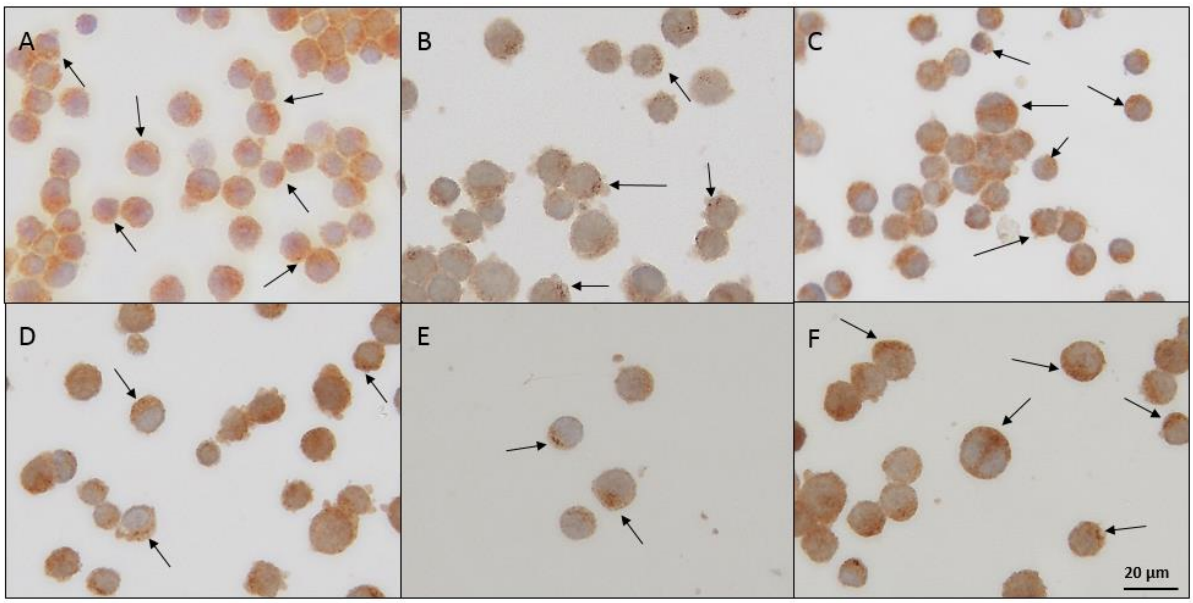

Figure 15: Immunohistochemical staining of ID-1 (1:750) in the P-STS cell lines. All samples express ID-1. Arrows mark the positive stained cells. A= WT, B= BB, C= ID-1, D= scr, E = siA, F= siB; Bar= 20 µm.

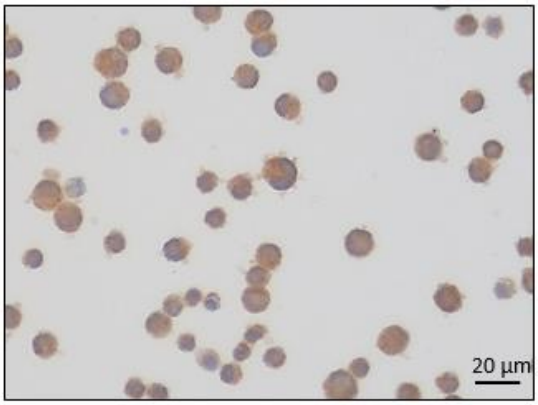

Figure 16: Negative control (rabbit IgG) of the IHC staining. Bar= 20 µm.

3.5.2.3 Immunofluorescence

Additionally, immunofluorescence with the same antibody (1:750) was performed, which led to similar results (Figure 17) as described previously (chapter 2.8.5.1). ID-1 was expressed in all samples. The silencing P-STS samples showed a lower ID-1 signal (Figure 17-E-F) compared to the scrambled control (Figure 17-D). The negative control (rabbit IgG) lacked the signal of the primary antibody (Figure 18). All pictures were taken with the same setup.

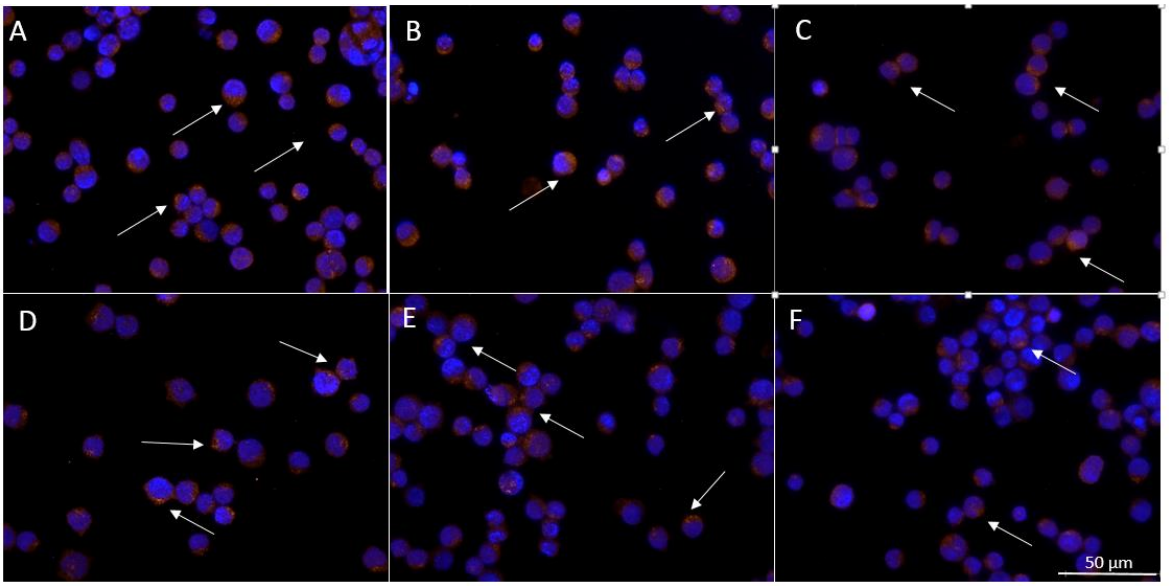

Figure 17: Immunofluorescence staining of ID-1 (1:750) in transduced P-STS cells. Arrows mark ID-1 positive stained cells. ID-1 is expressed in all samples. The silenced P-STS cells show a lower ID-1 signal. Red= ID-1, blue= DAPI, A= WT, B= BB, C= ID-1, D= scr, E= siA, F= siB; Bar= 50 µm.

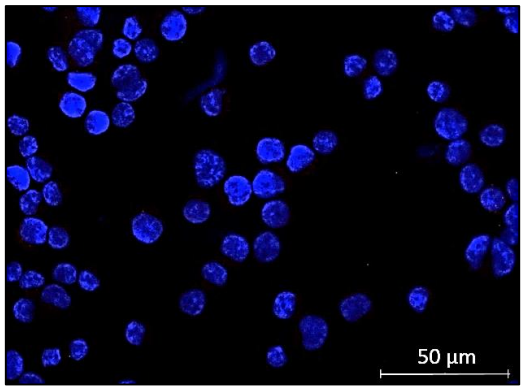

Figure 18: Negative control (normal rabbit IgG) of the ID-1 staining. No signal of the primary antibody was obtained. Red= ID-1, blue= DAPI; Bar= 50 µm.

3.6 Proliferation, viability and apoptosis assays

3.6.1 Proliferation measurement

Starting from a cell concentration of $2x10^5$ cells/mL in full medium the cell number was daily counted over three days with CASY©. Empty vectors did not significantly affect the proliferation of P-STS (Figure 19-A). Cells transduced with siA and siB had a similar proliferation curve as the scr transduced cells (Figure 19-B). The overexpression of ID-1 had no influence on the growth behavior of P-STS cells (Figure 19-C). At the end of the experiment all samples reached a cell number of approximately $4x10^5$ cells/mL.

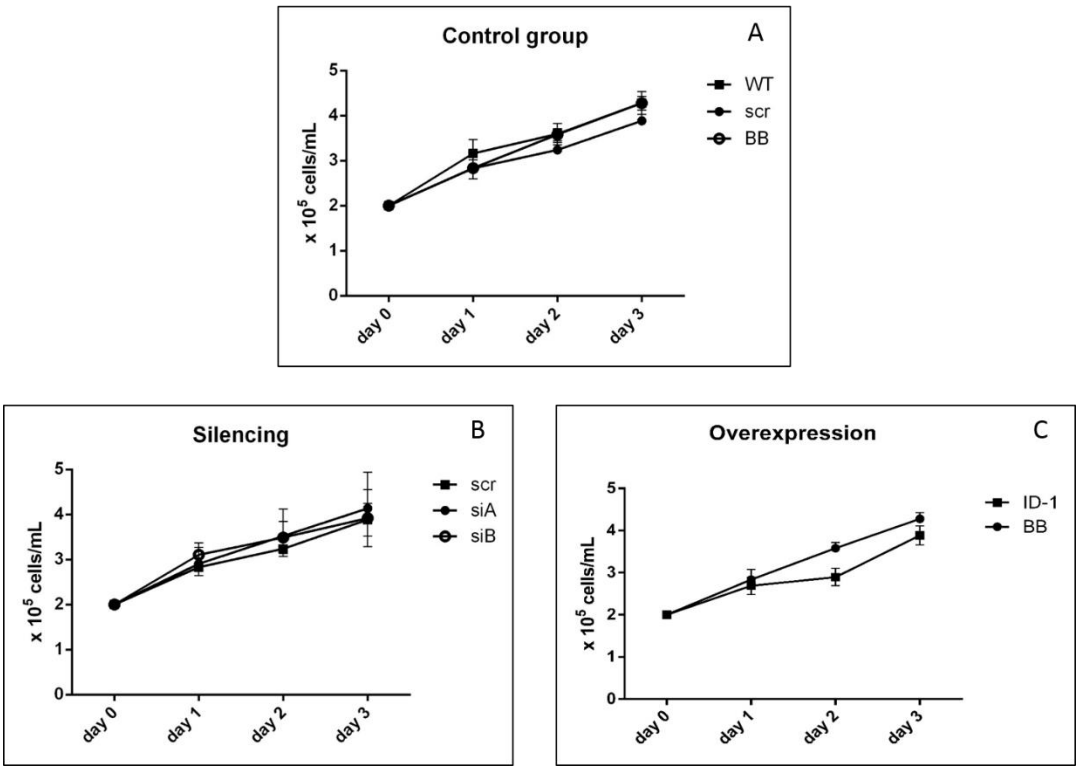

Figure 19: Growth curve of transduced P-STS cells. Starting with a concentration of $2x10^5$ cells/mL, all transduced P-STS cells reached approximately $4x10^5$ cell/mL. Slight differences in the cell number of the overexpressing sample were obtained at day two. A= control group, B= loss-of-function experiment, C= gain-of-function experiment. All datasets represent mean and SEM (n=4).

3.6.2 Viability assay

The viability of the cells was examined with WST-1 assay. Cells were observed over three days. After incubation with WST-1 for 60 min the absorbance was measured at 450 nm and the results were normalized to the proper control. On the third day of culturing the P-STS cells harboring the control vectors (BB and scr) showed higher viability than the wild type (Figure 20-A). The silencing variant B transduced cells had higher viability compared to the proper control over all days, whereas siA had slightly higher viability starting on day 2 (Figure 20-B). An increased viability was obtained on day 1 of the experiment from the ID-1 overexpressing cells compared with the empty vector. On day 2 and 3 the overexpression and the backbone transduced cells showed the same viability (Figure 20-C).

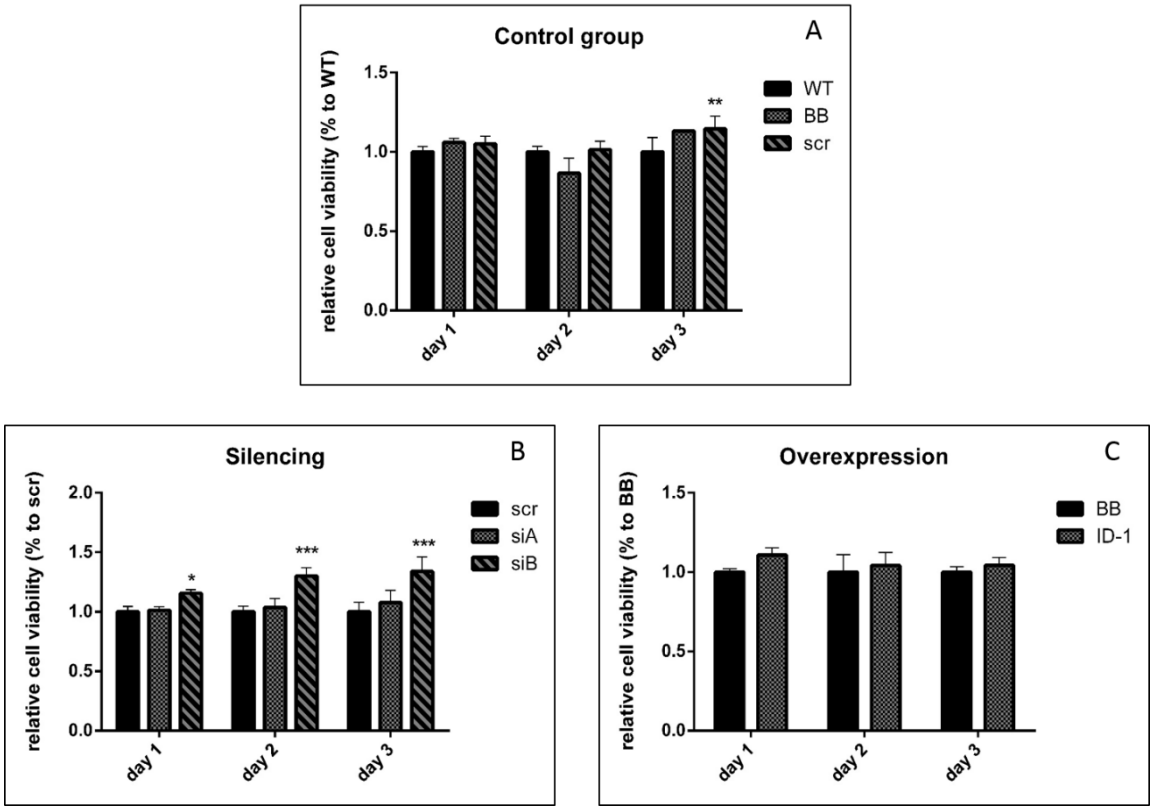

Figure 20: WST-1 assay of the transduced P-STS cell line. The controls had compared to the wild type, a higher viability on day 3. On day 1 and 2 no significant changes in the control group were measurable. The silencing samples had higher viability than the proper control. The cells, which overexpress ID-1 have a slight increase of viability on the first day. A= control group, B= loss-of-function experiment, C= gain-of-function experiment. All datasets (mean and SEM; n=3) were normalized to their proper control.

3.6.3 Apoptosis assay

Caspase 3/7 activation is a reliable indicator for cell apoptosis. The scrambled and the backbone control samples had a significant reduction of caspase 3/7 activity (Figure 21-A), whereas the same activity was obtained compared to the silencing constructs siA and siB (Figure 21-B) over three days. Overexpression of ID-1 led to less caspase 3/7 activity compared to the empty backbone control (Figure 21-C) over two days.

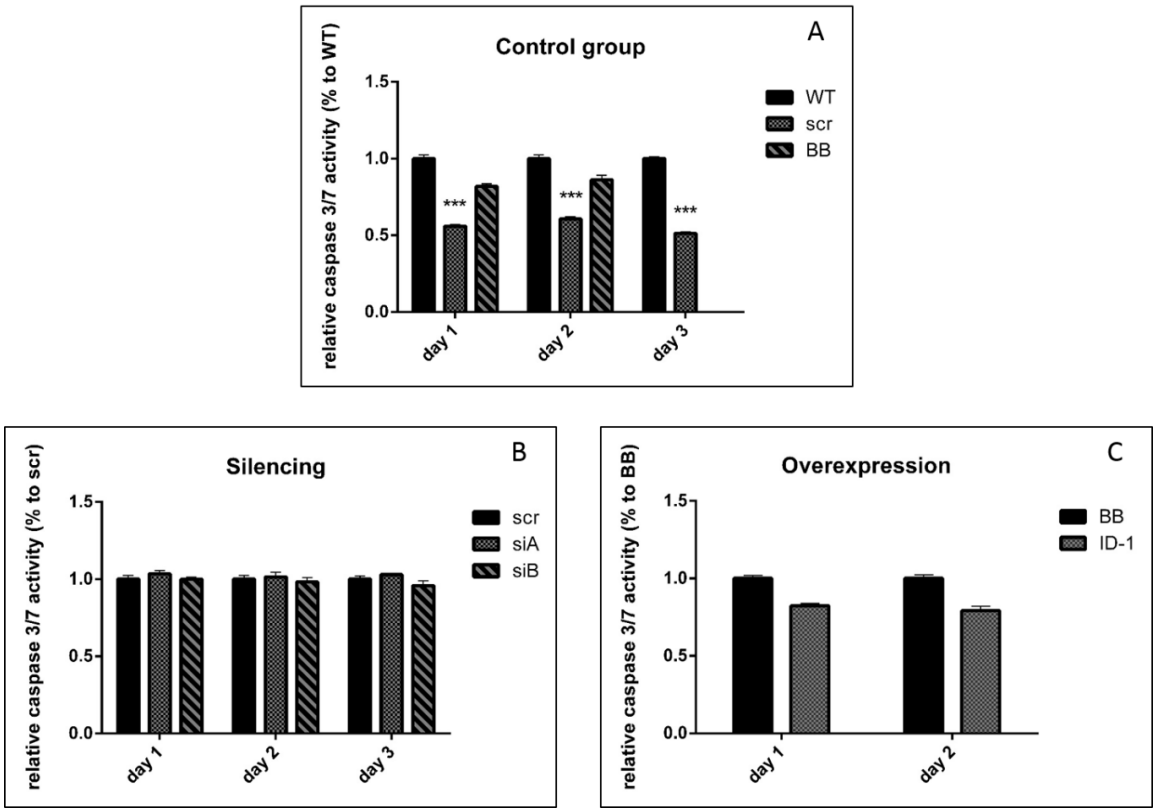

Figure 21: Caspase 3/7 assay of the transduced P-STS cells. The scr transduced cells had significant reduction of caspase 3/7 activity compared to the wild type. No differences in caspase 3/7 activity were obtained of the silencing experiment. Overexpressing of ID-1 led to less caspase 3/7 activity normalized to the BB control over two days. The BB control had less caspase 3/7 activity than the wild typ. A= control group, B= loss-of-function experiment, C= gain-of-function experiment. All datasets (mean and SEM, n= 3 for loss-of-function, n=1 for gain-of-function) were normalized to their proper control.

3.7 Tumor formation

3.7.1 *In vitro* tumor spheroid formation

Single P-STS cells were cultivated in ultra-low attachment plates for one week and *in vitro* formation of tumor spheroids was observed. Neither absence of ID-1 nor the overexpression did affect the spheroid formation. All samples had the ability to form dense tumor spheroids (Figure 22).

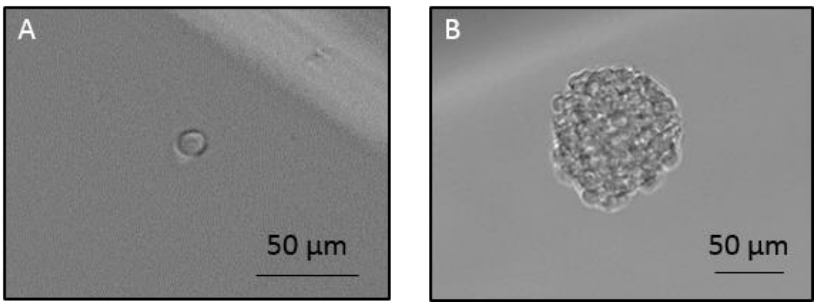

Figure 22: *In vitro* tumor spheroid formation. Within one week all transduced P-STS cells were able to form tumor spheroids starting out of one single cell (n=3). This picture is representative. A= single cell, B= tumor spheroid; Bar= 50 µm.

3.7.2 *In vivo* tumor formation assay

The xenografts were observed after three days of cultivation of $1x10^6$ P-STS cells on the chorioallantoic membrane (CAM) of the developing chicken. Two different types of tumor formation could be distinguished: the dense form (Figure 23) and the plane (Figure 24) form.

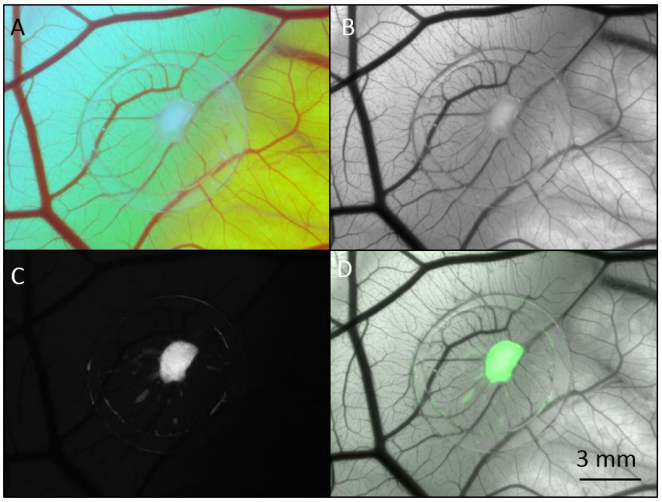

Figure 23: A representative xenograft of a dense tumor formation of $1x10^6$ transduced cells on the CAM. A= bright-field, B= black and white, C= fluorescence (GFP), D= merge; Bar= 3 mm.

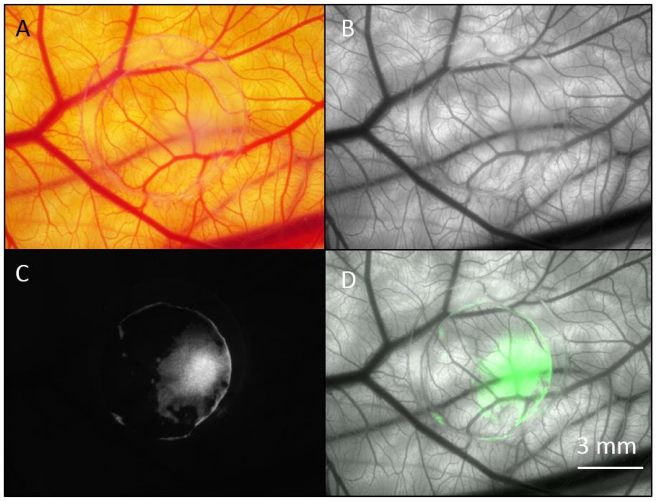

Figure 24: A representative xenograft of a plane tumor formation of $1x10^6$ transduced cells on the CAM. A= bright-field, B= black and white, C= fluorescence (GFP), D= merge; Bar= 3 mm.

All samples, except siA, were able to form both types of tumors. P-STS cells transduced with the silencing construct siA were only able to form spread plane tumors (n=8).

In total, 40 CAM assays were performed. For the scr and siB samples, 14 CAM assays were used, which had seven plane and seven dense tumor formations. The overexpression of ID-1 and its control had the tendency to form dense tumors in three CAM experiments (Figure 25).

Table 15: Numbers of CAM experiments and their type of tumor formation.

Sample	Dense tumor	Plane tumor	∑
BB	2	1	3
ID-1	2	1	3
scr	7	7	14
siA	0	8	8
siB	7	7	14

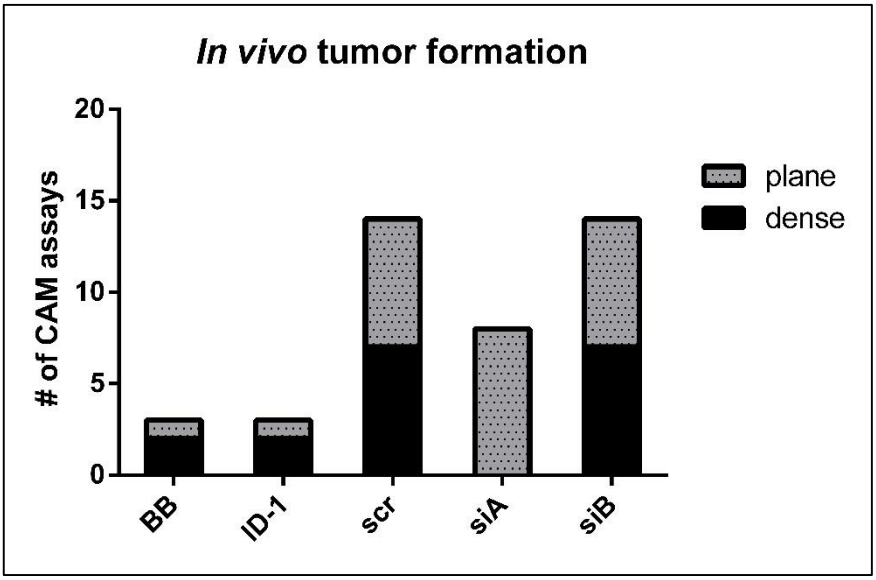

Figure 25: Schematic outcome of the CAM experiments regarding to *in vivo* tumor formation. All samples, except siA, were able to form dense and plane tumors on the CAM after three days.

Additionally, after excision, dehydration, paraffin embedding and cutting, the GFP expressing P-STS wild type had invasive characteristics (Figure 26-Arrows) and remained GFP active (Figure 26-B). Visualization of the CAM was done using rhodamine labeled *Lens culinaris* agglutinin (LCA; 1:500) staining (Figure 26–C).

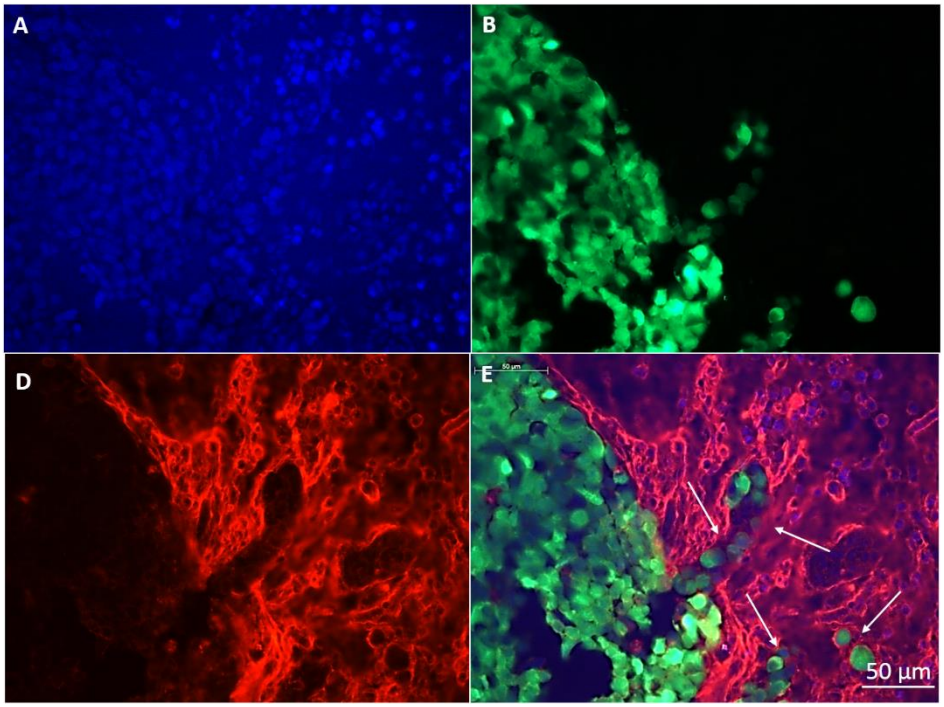

Figure 26: GFP expressing P-STS cells grew invasive on CAM. $1x10^6$ GFP tagged P-STS cells invaded the CAM after three days and remained active GFP after histological processing. Arrows mark invaded cells. A= DAPI, B= P-STS (GFP), C= LCA (1:500), D= merge; Bar= 50 µm.

4 Discussion

ID-1 is one of four members of the HLH transcription factor family and is highly linked to tumorigenesis and cancer biology, when dysregulated[12]. It has been shown that ID-1 is overexpressed in several types of cancer and this is strongly associated with invasion, angiogenesis and hence aggressiveness as well as chemotherapeutic resistance[14]. These characteristics lead to the connection between ID proteins and CSC[38]. In GEP-NETs the role of ID-1 in "stem-cell-ness" is not explored yet.

Previous studies in our lab proved the presence of CSC in the GEP-NET cell line P-STS. Moreover, we found the upregulation of ID-1 when P-STS cells were forced to grow three-dimensionally.

In this work, we studied the impact of ID-1 on "stem-cell-ness" characteristics of the P-STS cell line, which is heterogenic in phenotype and grows semi-adherent. Stained (DAPI, hematoxylin) P-STS nuclei appear diverse in size and shape: The cells which are in suspension state have smaller, round nuclei, whereas the adherent cells have bigger ones (Figure 15 and Figure 17).

4.1 Manipulation of the ID-1 expression

Gain-of-function and loss-of-function experiments are two common approaches to assess the biological function of proteins. In this work P-STS cells were transduced with ID-1 silencing and overexpressing lentiviruses and with corresponding control constructs (Appendix 7.2).

First, the constructs were transfected into HEK 293T cells, which produced the viral particles. As seen in Figure 10, almost all HEK 293T cells started expressing GFP after two rounds of transfection. Second, the P-STS cells were transduced with the collected virus particles, which resulted in GFP positive P-STS cells (Figure 11). According to the FACS analysis (Table 13) the efficiency of the transduction was low. Therefore, P-STS cells were subsequently treated with puromycin, which led to a significant enrichment of transduced cells (Table 14).

Quantification of ID-1 mRNA levels of the transduced cells was examined by qPCR. Unexpectedly, the scramble control and the backbone control constructs appeared to slightly influence the ID-1 expression on mRNA level (Figure 13–A). After intensive bioinformatical research we found that the siRNA sequence of the scr construct has six identic alignments with the sequence among the human genome (Ensembl)[57]. Therefore, we believe that the expressed scrambled siRNA may interact with an unknown mRNA and would not serve as a perfect control construct. However, both silenced P-STS cells had a statistically significant ($p<0.0001$) decrease of ID-1 mRNA compared with the scr control (Figure 13-B). On the other hand, ID-1 level of P-STS cells induced with the ID-1 overexpression construct were fourfold increased ($p<0.05$, Figure 13-C).

These results indicate that silencing and overexpression of ID-1 in P-STS cells were successful on mRNA level.

Since protein expression is a highly regulated process within the cell it is necessary to confirm the findings at protein level. The quantitative analysis of ID-1 was done with Western blot and immunohistological stainings were performed to visualize the subcellular localization of ID-1 in the P-STS cell line.

The quantitative analysis of Western blots turned out to be rather challenging:

First, ID-1 has a calculated molecular weight of 16 kDa using the Expert Protein Analysis System portal ExPASY[58]. In this study an ID-1 signal was obtained at 25 kDa. ID-1 has no recognition sequences for posttranslational modifications, which excludes phosphorylation and glycosylation as possible reasons for the size differences. Bounpheng *et al.* reported that ID proteins are so called short-time proteins with a halftime of 10-20 min before degradation *via* the ubiquitin-proteasome complex[59]. One ubiquitin molecule has a molecular weight of 8.5 kDa. Therefore, mono-ubiquitinated ID-1 would have a mass of 24.5 kDa, which corresponds to the detected mass.

Second, due to technical problems, the results were inconsistent. In the silencing experiments, a twofold reduction of ID-1 protein levels was obtained (Figure 14–B), however, the ID-1 overexpression could not be verified by Western blot and needs to be repeated (Appendix 7.6). Additionally, enrichment of ID-1 protein with immunoprecipitation would be helpful to overcome the technical problems and to confirm the possible interaction of ID-1 with the ubiquitin-proteasome complex.

The immunostaining of P-STS cells (Figure 15 and Figure 17) showed that ID-1 protein is rather localized in the cytoplasm than in the nucleus. In addition, dividing cells appeared to have a higher ID-1 signal than not dividing cells, probably because of the specific role of ID-1 and its upregulation during cell cycle. These localizations are according to the "Universal Protein Resource"[60] (accession number: P41134), however, we noticed different expression levels within one sample (Figure 17). The obvious explanation could be that our experiments were performed with a mixed population of transduced cells. They have a heterogeneity in the sites of construct insertion and therefore express ID-1 at different levels.

The number of insertions led, for instance, to inconsistent siRNA expression levels within the population of transduced P-STS cells. Flow cytometric analysis of the GFP expression confirmed this assumption (Appendix 7.4). To overcome the heterogeneity FACS sorted cells should be used for further experiments.

Nevertheless, we detected a higher ID-1 signal in ID-1 overexpressing cells compared to BB control (Figure 15-C and Figure 17-C).

Taken together so far, manipulation of ID-1 expression in the P-STS cell line was successful. From that we were able to investigate the effects of ID-1 on the P-STS cell line with subsequent experiments.

4.2 Role of ID-1 in P-STS cell proliferation and cell viability

CASY© cell counting was performed to measure the proliferation of the transduced cells. After three days of cultivation the samples reached $4x10^6$ cells/mL but only slight differences were obtained (Figure 19):

P-STS cells overexpressing ID-1, for instance, showed a minor increase of proliferation after two days compared to the P-STS transduced with BB control construct (Figure 19-C). The silencing of ID-1 did not affect the proliferation of P-STS at all (Figure 19-B), whereas the scrambled control showed a slight decrease in cell number (Figure 19-A). Proliferation analysis of the P-STS cell line with an additional method could provide more insights, as Guo *et al.* showed that proliferation of the U87 cell line is dependent of ID-1 expression using BrdU assay[61]. Moreover, since proliferation is dependent on the FBS concentration in the culturing medium, it is obvious that high FBS concentration influence the cells by supplementing them with growth factors. Therefore, cell counting in low serum medium should be performed to avoid the extrinsic growth factors.

The activity of mitochondrial enzymes, which corresponds to the viability[62] was measured *via* WST-1 assay. P-STS cells transduced with siB had a significant ($p<0.0001$) higher viability than the scr control, whereas siA transduced cells showed nearly the same viability (Figure 20).

Probably the two isoforms (ID-1a and ID-1b) could have a competitive impact on viability of the P-STS cell line. ID-1a (155 amino acids) and ID-1b (149 amino acids)[63] differ in their C-terminal sequences, which is associated with their specificity to interact with proteins. In lung cancer, for instance, ID-1b is more connected to malignancy of the tumor than ID-1a[64]. Manrique *et al.* showed that overexpression of ID-1a enhances proliferation, whereas overexpressing ID-1b inhibits this and preserves an undifferentiated cancer stem cell like state in murine colon cancer[65]. In our study, Western blot analysis showed a higher silencing effect for the smaller isoform (ID-1b). The ID-1b band of the siA transduced P-STS had decreased intensity compared with the ID-1b band of siB sample (Figure 14-B). In addition, the ID-1a bands showed equal intensity. This led us to claim that ID-1b has a higher impact on the viability of the P-STS cell line strengthened by the fact that scr and siA had the same viability. To investigate this aim, it is necessary to suppress both isoforms of ID-1 independently. Tanaka *et al.*

showed that overexpression of ID-1 does not affect the viability of neonatal myocytes, fibroblast, vascular smooth muscle cells or endothelial cells within five days[66].

Our findings indicate that on the first day of the experiment overexpression of ID-1 led to slightly higher viability in the P-STS cells, whereas, after three days, the viability of the control was equal to the overexpression (Figure 20-C).

Cell proliferation is ID-1 independent and manipulating ID-1 expression had a slight impact on the viability of the P-STS cell line.

4.3 Role of ID-1 in P-STS cell death

Caspase 3/7 activity was measured as indicator for apoptosis within the samples. The results of this work showed that apoptosis is independent of ID-1 silencing (Figure 21-B). In contrast, overexpression of ID-1 led to decreased caspase 3/7 activity (Figure 21-C). In addition, scr ($p<0.0001$) and BB samples had lower caspase 3/7 activity than the WT (Figure 21-A). These findings indicate that transduced P-STS cells show less apoptosis than the WT. Tanaka *et al.* described the induction of apoptosis in neonatal myocytes due to ID-1 overexpression[66]. Our results demonstrate the opposite in the P-STS cell line. The differences can be explained with the different types of cells. Tanaka *et al.* described the influence of ID-1 on not immortalized muscle cells, whereas the subject of our study was a neuroendocrine tumor cell line. In addition, the used assays were based on different principles: Tanaka *et al.* used TUNEL assay, to detect apoptotic cells microscopically and we performed substrate cleavage based luminescence measurements.

Silencing of ID-1 in the P-STS cell line did not influence apoptosis since lacking one single protein within the cell might not affect the whole complex machinery of cell death. The absence or lower expression of one protein forces the cell to utilize other pathways. Therefore, redundant proteins, which may reverse the biological effect, might substitute the missing one. Chen *et al.* showed that downregulation of ID-1 had less effects on small cell lung carcinoma cell line N417 than suppressing ID-1 and ID-3 simultaneously[67]. In addition, Shuno *et al.* investigated the role of ID-1/ID-3 double knockouts on the metastatic potential in pancreatic cancer[68]. Furthermore, studies of Sharma *et al.* revealed that ID-1 and ID-3 are controlling CDKs independently. Hence, expression of ID-3 is not influenced by the expression of ID-1 directly and *vice versa*. Although these ID proteins are targeting different proteins, their biological effects are analogous[69].

Therefore, ID-3 levels in the newly generated ID-1 manipulated P-STS cell lines should be determined. If there is an unknown existing redundancy in the P-STS cell line of ID-1 and ID-3, ID-3 should be

upregulated in the ID-1 silenced cells as well as downregulated in the samples which overexpress ID-1.

To investigate the redundancy of ID-1 and ID-3, it would be obligatory to create a co-suppression of both ID proteins in the P-STS cell line.

In summary, apoptosis appears to be independent of silencing ID-1 in the P-STS cell line and in contrast, overexpression of ID-1 led the P-STS cells to be less prone to apoptosis.

4.4 ID-1 in P-STS cell self-renewal and tumor formation

Cultivating the transduced P-STS cells under special tumor formation conditions forced the cells to grow three dimensional. Both ID-1 overexpressing and silenced P-STS cells were able to form tumor spheroids *in vitro* originating from one single cell (Figure 22). Barrett *et al.* were able to show that murine glioma cancer stem cells with high levels of expressed ID-1 have high self-renewal capacity, whereas low ID-1 expressing glioma CSCs have proliferative potential with limited self-renewal capacity. Interestingly, cells which express low levels of ID-1 were able to generate tumors in mice more rapidly[70].

All P-STS cell lines grafted on the chicken chorioallantoic membrane formed distinct tumors. CAM revealed the tumor formation capacity of transduced P-STS cells *in vivo.* This experiment showed that ID-1 overexpressing P-STS cells had a tendency to form dense tumors and that silencing ID-1 had an impact of *in vivo* dense tumor formation within three days (Figure 25).

The silenced version B as well as the scr control formed equal numbers of plane and dense tumors, whereas, siA only formed plane tumors. As mentioned above the crosstalk between ID-1 and ID-3 as well as the effects of the two ID-1 isoforms are plausible reasons for these observations.

According to the findings of Barrett *et al.* ID-1 might play a role in the initiation of tumor formation[70]. Therefore, it would be interesting to observe the behavior of transduced P-STS cell in tumor formation *in vitro* as *in vivo* within a shorter incubation time.

As shown in Figure 26, GFP expressing P-STS cells grow invasive on the CAM. In addition to *in vivo* tumor formation, the invasiveness of the silencing and overexpressing samples has to be determined. Therefore, the harvested specimen have to be dehydrated and paraffin embedded, as well as cut and immunohistochemically stained for specific GEP-NET markers, such as synaptophysin or chromogranin A in future experiments.

Taken all findings together, we are able to say that ID-1 slightly influences the cancer stem cell characteristics of the P-STS cell line. For the characterization of ID-1 as CSC marker in the P-STS cell line, the impact of gain and function has to be more distinct than observed.

5 Conclusion

This work explores the role of ID-1 in the "stem-cell-ness" of GEP-NET cell line P-STS. Within this study I successfully established a protocol for the transduction of P-STS cells as well as subsequent quantification methods of ID-1 expression. Although the ID-1 gain-of-function and loss-of-function only slightly affected the "stem-cell-ness"-related properties examined here (*e.g.* self-renewal and tumor spheroid formation) the established cell lines represent excellent tools for studying further impacts of the interaction of ID-1 in the poorly understood pathophysiology of gastroenteropancreatic neuroendocrine tumors.

6 References

1. DeLellis, R. A. The neuroendocrine system and its tumors: an overview. *Am. J. Clin. Pathol.* **115 Suppl,** 5–16 (2001).

2. Adler, D. G. Neuroendocrine Tumors: Review and Clinical Update. *Hosp. Physician* 12–21 (2007).

3. Kaltsas, G. A., Besser, G. M. & Grossman, A. B. The diagnosis and medical management of advanced neuroendocrine tumors. *Endocr. Rev.* **25,** 458–511 (2004).

4. Oberg, K. Neuroendocrine tumors of the gastrointestinal tract: recent advances in molecular genetics, diagnosis, and treatment. *Curr. Opin. Oncol.* **17,** 386–391 (2005).

5. Yao, J. C. *et al.* One Hundred Years After 'Carcinoid': Epidemiology of and Prognostic Factors for Neuroendocrine Tumors in 35,825 Cases in the United States. *J. Clin. Oncol.* **26,** 3063–3072 (2008).

6. Modlin, I. M. *et al.* Gastroenteropancreatic neuroendocrine tumours. *Lancet Oncol.* **9,** 61–72 (2008).

7. Wiedenmann, B., John, M., Ahnert-Hilger, G. & Riecken, E. O. Molecular and cell biological aspects of neuroendocrine tumors of the gastroenteropancreatic system. *J. Mol. Med. (Berl).* **76,** 637–647 (1998).

8. Ellis, H. M., Spann, D. R. & Posakony, J. W. Extramacrochaetae, a negative regulator of sensory organ development in Drosophila, defines a new class of helix-loop-helix proteins. *Cell* **61,** 27–38 (1990).

9. Garrell, J. & Modolell, J. The Drosophila extramacrochaetae locus, an antagonist of proneural genes that, like these genes, encodes a helix-loop-helix protein. *Cell* **61,** 39–48 (1990).

10. Deed, R. W., Hirose, T., Mitchell, E. L., Santibanez-Koref, M. F. & Norton, J. D. Structural organisation and chromosomal mapping of the human Id-3 gene. *Gene* **151,** 309–314 (1994).

11. Mathew, S., Chen, W., Murty, V. V, Benezra, R. & Chaganti, R. S. Chromosomal assignment of human ID1 and ID2 genes. *Genomics* **30,** 385–387 (1995).

12. Ruzinova, M. B. & Benezra, R. Id proteins in development, cell cycle and cancer. *Trends Cell Biol.* **13,** 410–418 (2003).

13. Pesce, S. & Benezra, R. The loop region of the helix-loop-helix protein Id1 is critical for its dominant negative activity. *Mol. Cell. Biol.* **13,** 7874–7880 (1993).

14. Perk, J., Iavarone, A. & Benezra, R. Id family of helix-loop-helix proteins in cancer. *Nat. Rev. Cancer* **5,** 603–614 (2005).

15. Norton, J. D. ID helix-loop-helix proteins in cell growth, differentiation and tumorigenesis. *J. Cell Sci.* **113,** 3897–3905 (2000).

16. Hollnagel, A., Oehlmann, V., Heymer, J., Rüther, U. & Nordheim, A. Id genes are direct targets of bone morphogenetic protein induction in embryonic stem cells. *J. Biol. Chem.* **274,** 19838–19845 (1999).

17. Korchynskyi, O. & Ten Dijke, P. Identification and functional characterization of distinct critically important bone morphogenetic protein-specific response elements in the Id1 promoter. *J. Biol. Chem.* **277,** 4883–4891 (2002).

18. Cubillo, E. *et al.* E47 and Id1 Interplay in Epithelial-Mesenchymal Transition. *PLoS One* **8,** 1–10 (2013).

19. López-Rovira, T., Chalaux, E., Massagué, J., Rosa, J. L. & Ventura, F. Direct binding of Smad1 and Smad4 to two distinct motifs mediates bone morphogenetic protein-specific transcriptional activation of Id1 gene. *J. Biol. Chem.* **277,** 3176–3185 (2002).

20. Kang, Y., Chen, C.-R. & Massagué, J. A Self-Enabling TGFβ Response Coupled to Stress Signaling: Smad Engages Stress Response Factor ATF3 for Id1 Repression in Epithelial Cells. *Mol. Cell* **11,** 915–926 (2003).

21. Valdimarsdottir, G. *et al.* Stimulation of Id1 expression by bone morphogenetic protein is sufficient and necessary for bone morphogenetic protein-induced activation of endothelial cells. *Circulation* **106,** 2263–2270 (2002).

22. Hacker, C. *et al.* Transcriptional profiling identifies Id2 function in dendritic cell development. *Nat. Immunol.* **4,** 380–386 (2003).

23. Yokota, Y. & Mori, S. Role of Id family proteins in growth control. *J. Cell. Physiol.* **190,** 21–28 (2002).

24. Ohtani, N. *et al.* Opposing effects of Ets and Id proteins on p16INK4a expression during cellular senescence. *Nature* **409,** 1067–1070 (2001).

25. Hara, E., Hall, M. & Peters, G. Cdk2-dependent phosphorylation of Id2 modulates activity of E2A-related transcription factors. *EMBO J.* **16,** 332–342 (1997).

26. Prabhu, S., Ignatova, A., Park, S. T. & Sun, X. H. Regulation of the expression of cyclin-dependent kinase inhibitor p21 by E2A and Id proteins. *Mol. Cell. Biol.* **17,** 5888–5896 (1997).

27. Kebebew, E., Treseler, P. a, Duh, Q. Y. & Clark, O. H. The helix-loop-helix transcription factor, Id-1, is overexpressed in medullary thyroid cancer. *Surgery* **128,** 952–957 (2000).

28. Bain, G. *et al.* Regulation of the helix-loop-helix proteins, E2A and Id3, by the Ras-ERK MAPK cascade. *Nat. Immunol.* **2,** 165–171 (2001).

29. Swarbrick, A. *et al.* Regulation of cyclin expression and cell cycle progression in breast epithelial cells by the helix-loop-helix protein Id1. *Oncogene* **24,** 381–389 (2005).

30. Tournay, O. & Benezra, R. Transcription of the dominant-negative helix-loop-helix protein Id1 is regulated by a protein complex containing the immediate-early response gene Egr-1. *Mol. Cell. Biol.* **16,** 2418–2430 (1996).

31. Weisz, L. *et al.* Transactivation of the EGR1 gene contributes to mutant p53 gain of function. *Cancer Res.* **64,** 8318–8327 (2004).

32. Lyden, D. *et al.* Id1 and Id3 are required for neurogenesis, angiogenesis and vascularization of tumour xenografts. *Nature* **401,** 670–677 (1999).

33. Ruzinova, M. B. *et al.* Effect of angiogenesis inhibition by Id loss and the contribution of bone-marrow-derived endothelial cells in spontaneous murine tumors. *Cancer Cell* **4,** 277–289 (2003).

34. Fong, S. *et al.* Id-1 as a molecular target in therapy for breast cancer cell invasion and metastasis. *Proc. Natl. Acad. Sci. U. S. A.* **100,** 13543–13548 (2003).

35. Minn, A. J. *et al.* Genes that mediate breast cancer metastasis to lung. *Nature* **436,** 518–524 (2005).

36. Beck, B. & Blanpain, C. Unravelling cancer stem cell potential. *Nat Rev Cancer* **13,** 727–738 (2013).

37. Romero-Lanman, E. E., Pavlovic, S., Amlani, B., Chin, Y. & Benezra, R. Id1 Maintains Embryonic Stem Cell Self-Renewal by Up-Regulation of Nanog and Repression of Brachyury Expression. *Stem Cells and Development* **21,** 384–393 (2012).

38. Lasorella, A., Benezra, R. & Iavarone, A. The ID proteins: master regulators of cancer stem cells and tumour aggressiveness. *Nat. Rev. Cancer* **14,** 77–91 (2014).

39. O'Brien, C. A. *et al.* ID1 and ID3 Regulate the Self-Renewal Capacity of Human Colon Cancer-Initiating Cells through p21. *Cancer Cell* **21,** 777–792 (2012).

40. Gaur, P. *et al.* Identification of cancer stem cells in human gastrointestinal carcinoid and neuroendocrine tumors. *Gastroenterology* **141,** 1728–1737 (2011).

41. Marlies Hölzl. Identification and characterisation of neuroendocrine cancer stem cells in P-STS cell line. (Medical University of Graz, 2014).

42. Pfragner, R. *et al.* Establishment and characterization of three novel cell lines - P-STS, L-STS, H-STS - Derived from a human metastatic midgut carcinoid. *Anticancer Res.* **29,** 1951–1961 (2009).

43. Yu, E. Z., Li, Y.-Y., Liu, X.-H., Kagan, E. & McCarron, R. M. Antiapoptotic action of hypoxia-inducible factor-1 alpha in human endothelial cells. *Lab. Invest.* **84,** 553–561 (2004).

44. Locklin, R. M. *et al.* Assessment of gene regulation by bone morphogenetic protein 2 in human marrow stromal cells using gene array technology. *J. Bone Miner. Res.* **16,** 2192–2204 (2001).

45. Livak, K. J. & Schmittgen, T. D. Analysis of relative gene expression data using real-time quantitative PCR and the 2(-Delta Delta C(T)) Method. *Methods* **25,** 402–408 (2001).

46. Pfaffl, M. W. A new mathematical model for relative quantification in real-time RT-PCR. *Nucleic Acids Res.* **29,** e45 (2001).

47. Smith, P. K. *et al.* Measurement of protein using bicinchoninic acid. *Anal. Biochem.* **150,** 76–85 (1985).

48. Laemmli, U. K. Cleavage of Structural Proteins during the Assembly of the Head of Bacteriophage T4. *Nature* **227,** 680–685 (1970).

49. Haid, A. & Suissa, M. Immunochemical identification of membrane proteins after sodium dodecyl sulfate-polyacrylamide gel electrophoresis. *Methods Enzymol.* **96,** 192–205 (1983).

50. Schneider, C. a, Rasband, W. S. & Eliceiri, K. W. NIH Image to ImageJ: 25 years of image analysis. *Nat. Methods* **9,** 671–675 (2012).

51. Berridge, M., Tan, A., McCoy, K. & Wang, R. The biochemical and cellular basis of cell proliferation assays that use tetrazolium salts. *Biochemica* 4–9 (1996).

52. Bayascas, J. R., Yuste, V. J., Benito, E., Garcia-Fernandez, J. & Comella, J. X. Isolation of AmphiCASP-3/7, an ancestral caspase from amphioxus (Branchiostoma floridae). Evolutionary considerations for vertebrate caspases. *Cell Death Differ.* **9,** 1078–1089 (2002).

53. STEMCELL Technologies. Tumorsphere Culture of Human Breast Cancer Cell Lines. *Tech. Bull.* 1–4 (2014).

54. Deryugina, E. I. & Quigley, J. P. Chick embryo chorioallantoic membrane model systems to study and visualize human tumor cell metastasis. *Histochem.Cell Biol.* **130,** 1119–1130 (2008).

55. Cumming, G., Fidler, F. & Vaux, D. L. Error bars in experimental biology. *Journal of Cell Biology* **177,** 7–11 (2007).

56. Altschul, S. F., Gish, W., Miller, W., Myers, E. W. & Lipman, D. J. Basic local alignment search tool. *J. Mol. Biol.* **215,** 403–410 (1990).

57. Cunningham, F. *et al.* Ensembl 2015. *Nucleic Acids Res.* **43 ,** D662–D669 (2015).

58. Gasteiger, E. *et al.* ExPASy: The proteomics server for in-depth protein knowledge and analysis. *Nucleic Acids Res.* **31,** 3784–3788 (2003).

59. Bounpheng, M. A., Dimas, J. J., Dodds, S. G. & Christy, B. A. Degradation of Id proteins by the ubiquitin-proteasome pathway. *FASEB J.* **13,** 2257–2264 (1999).

60. Consortium, T. U. UniProt: a hub for protein information. *Nucleic Acids Res.* **43 ,** D204–D212 (2015).

61. Guo, P., Lan, J., Ge, J., Mao, Q. & Qiu, Y. ID1 regulates U87 human cell proliferation and invasion. *Oncol. Lett.* **6,** 921–926 (2013).

62. Mosmann, T. Rapid colorimetric assay for cellular growth and survival: application to proliferation and cytotoxicity assays. *J. Immunol. Methods* **65,** 55–63 (1983).

63. Nehlin, J. O., Hara, E., Kuo, W. L., Collins, C. & Campisi, J. Genomic organization, sequence, and chromosomal localization of the human helix-loop-helix Id1 gene. *Biochem. Biophys. Res. Commun.* **231,** 628–634 (1997).

64. Nguewa, P. *et al.* Id-1B, an alternatively spliced isoform of the inhibitor of differentiation-1, impairs cancer cell malignancy through inhibition of proliferation and angiogenesis. *Curr. Mol. Med.* **14,** 151–62 (2014).

65. Manrique, I. *et al.* The inhibitor of differentiation isoform Id1b, generated by alternative splicing, maintains cell quiescence and confers self-renewal and cancer stem cell-like properties. *Cancer Lett.* **356,** 899–909 (2015).

66. Tanaka, K. *et al.* Expression of Id1 results in apoptosis of cardiac myocytes through a redox-dependent mechanism. *J. Biol. Chem.* **273,** 25922–25928 (1998).

67. Chen, D., Forootan, S. S., Gosney, J. R. & Forootan, F. S. Increased expression of Id1 and Id3 promotes tumorigenicity by enhancing angiogenesis and suppressing apoptosis in small cell lung cancer. *Genes&Cancer* **5,** 5–6 (2014).

68. Shuno, Y. *et al.* Id1/Id3 Knockdown Inhibits Metastatic Potential of Pancreatic Cancer. *J. Surg. Res.* **161,** 76–82 (2010).

69. Sharma, P., Patel, D. & Chaudhary, J. Id1 and Id3 expression is associated with increasing grade of prostate cancer: Id3 preferentially regulates CDKN1B. *Cancer Med.* **1,** 187–197 (2012).

70. Barrett, L. E. *et al.* Self-Renewal Does Not Predict Tumor Growth Potential in Mouse Models of High-Grade Glioma. *Cancer Cell* **21,** 11–24 (2012).

7 Appendix

7.1 Buffers

1x PBS (pH 7,4)	
NaCl	8 g
KCl	0.3 g
KH_2PO_4	2 mg
$Na_2HPO_4 \bullet 2\ H_2O$	10 mg
Protein lysis buffer	
TRIS base (50 mM)	60.75 mg
EDTA (10 mM)	37.22 mg
Triton X-100 (1%) or NP-40	100 µL
Inhibitor cocktail solution	10 µL
1x Running buffer (pH 8.3)	
TRIS	3 g
Glycin	1.4 g
SDS	1 g
Transfer buffer (1 L)	
Methanol (20%)	200 mL
Running Buffer (TRIS, Glycin, SDS)	100 mL
H_2O	700 mL
1x TBS-T (pH 7.4)	
NaCl	8.8 g
KCl	0.2 g
TRIS base	3.0 g
Tween® 20	1 mL

7.2 Constructs maps

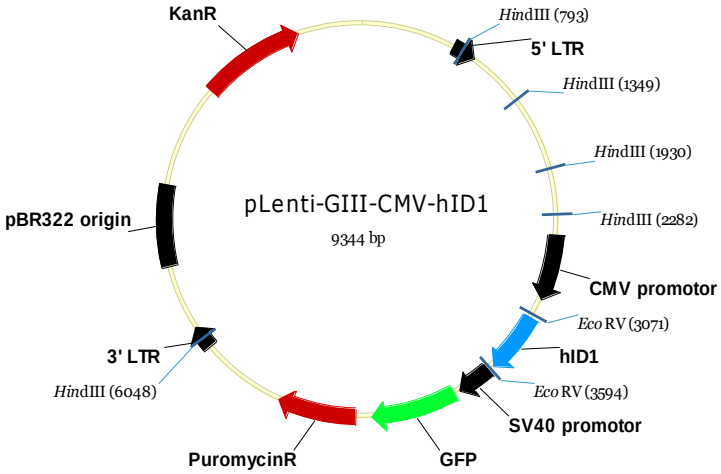

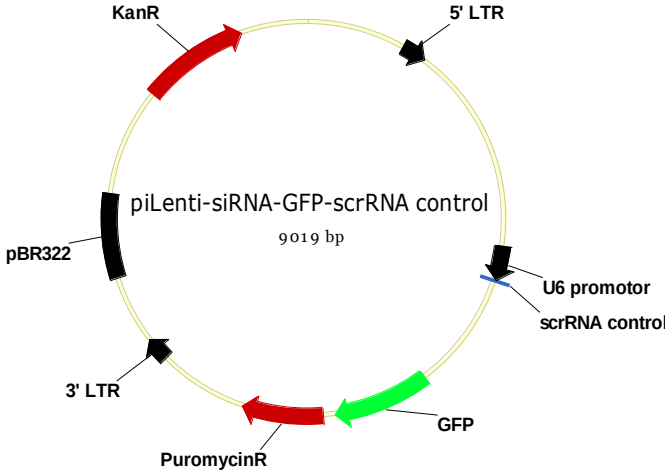

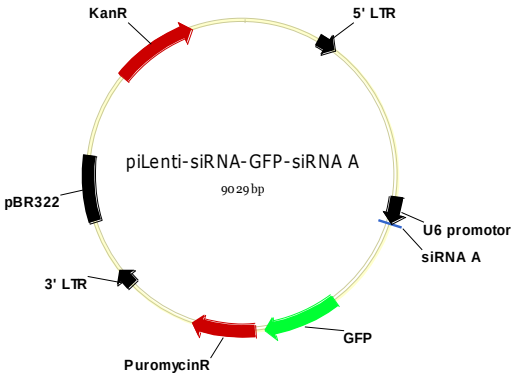

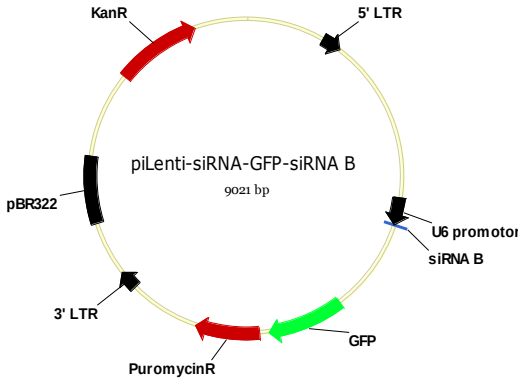

7.3 Sequencing alignments and electropherograms

7.3.1 ID-1 overexpression

```
                          EcoRV                                  ID-1->
ID-1-Construct  AGCTAGCGATATCAACAAGTTTGTACAAAAAAGTTGGCATGAAAGTCGCCAGTGGCAGCA
2_ID1_CMV-for   AGCTAGCGATATCAACAAGTTTGTACAAAAAAGTTGGCATGAAAGTCGCCAGTGGCAGCA
                ************************************************************

ID-1-Construct  CCGCCACCGCCGCCGCGGGCCCCAGCTGCGCGCTGAAGGCCGGCAAGACAGCGAGCGGTG
2_ID1_CMV-for   CCGCCACCGCCGCCGCGGGCCCCAGCTGCGCGCTGAAGGCCGGCAAGACAGCGAGCGGTG
                ************************************************************

ID-1-Construct  CGGGCGAGGTGGTGCGCTGTCTGTCTGAGCAGAGCGTGGCCATCTCGCGCTGCGCCGGGG
2_ID1_CMV-for   CGGGCGAGGTGGTGCGCTGTCTGTCTGAGCAGAGCGTGGCCATCTCGCGCTGCGCCGGGG
                ************************************************************

ID-1-Construct  GCGCCGGGGCGCGCCTGCCTGCCCTGCTGGACGAGCAGCAGGTAAACGTGCTGCTCTACG
2_ID1_CMV-for   GCGCCGGGGCGCGCCTGCCTGCCCTGCTGGACGAGCAGCAGGTAAACGTGCTGCTCTACG
                ************************************************************

ID-1-Construct  ACATGAACGGCTGTTACTCACGCCTCAAGGAGCTGGTGCCCACCCTGCCCCAGAACCGCA
2_ID1_CMV-for   ACATGAACGGCTGTTACTCACGCCTCAAGGAGCTGGTGCCCACCCTGCCCCAGAACCGCA
                ************************************************************

ID-1-Construct  AGGTGAGCAAGGTGGAGATTCTCCAGCACGTCATCGACTACATCAGGGACCTTCAGTTGG
2_ID1_CMV-for   AGGTGAGCAAGGTGGAGATTCTCCAGCACGTCATCGACTACATCAGGGACCTTCAGTTGG
                ************************************************************

ID-1-Construct  AGCTGAACTCGGAATCCGAAGTTGGAACCCCCGGGGGCCGAGGGCTGCCGGTCCGGGCTC
2_ID1_CMV-for   AGCTGAACTCGGAATCCGAAGTTGGAACCCCCGGGGGCCGAGGGCTGCCGGTCCGGGCTC
                ************************************************************

ID-1-Construct  CGCTCAGCACCCTCAACGGCGAGATCAGCGCCCTGACGGCCGAGGCGGCATGCGTTCCTG
2_ID1_CMV-for   CGCTCAGCACCCTCAACGGCGAGATCAGCGCCCTGACGGCCGAGGCGGCATGCGTTCCTG
                ************************************************************

ID-1-Construct  CGGACGATCGCATCTTGTGTCGCTGCCCAACTTTCTTGTACAAAGTGGTTGATATCTGAG
2_ID1_CMV-for   CGGACGATCGCATCTTGTGTCGCTGCCCAACTTTCTTGTACAAAGTGGTTGATATCTGAG
                ************************************************************
                                                              EcoRV
```

7.3.2 Scrambled control (scr)

```
                        end of U6 promoter          scr
scr_construct   TTGGCTTTATATATCTTGTGGAAAGGACAAAAAGGGTGAACTCACGTCAGAATTTTTTGG
5_scr_U6        TTGGCTTTATATATCTTGTGGAAAGGACAAAAAGGGTGAACTCACGTCAGAATTTTTTGG
                ************************************************************
```

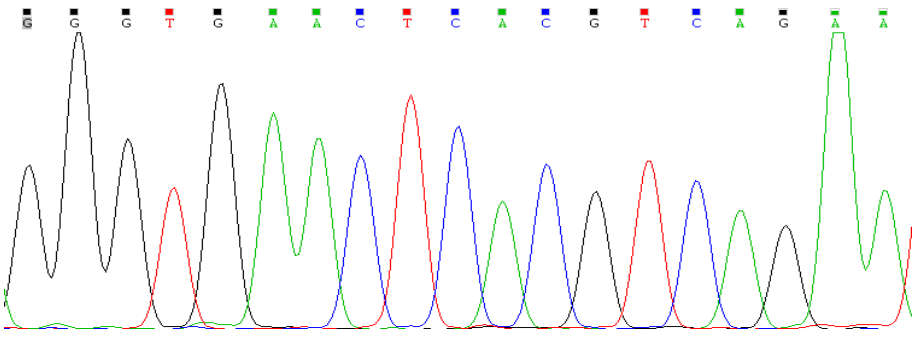

7.3.3 siRNA version A (siA)

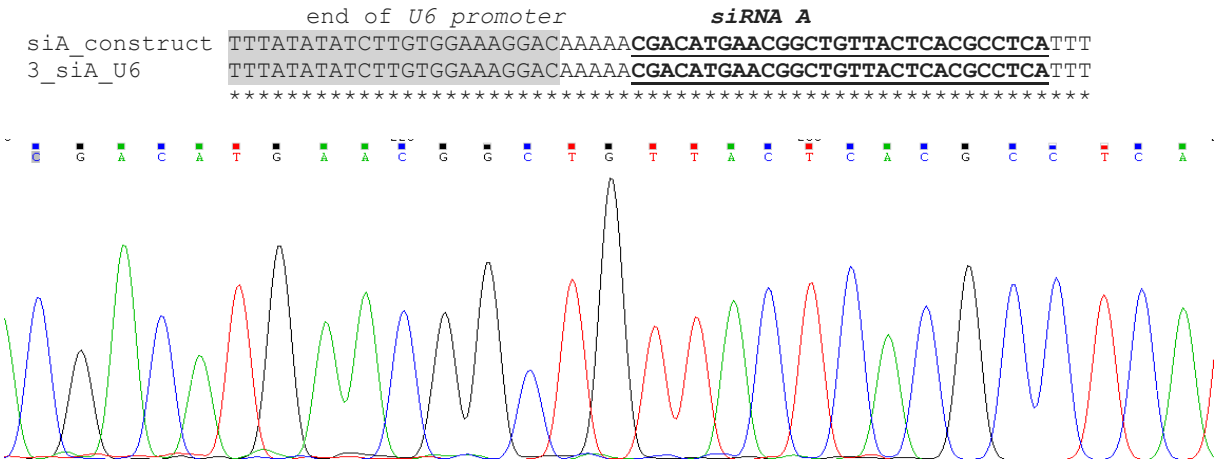

7.3.4 siRNA version B (siB)

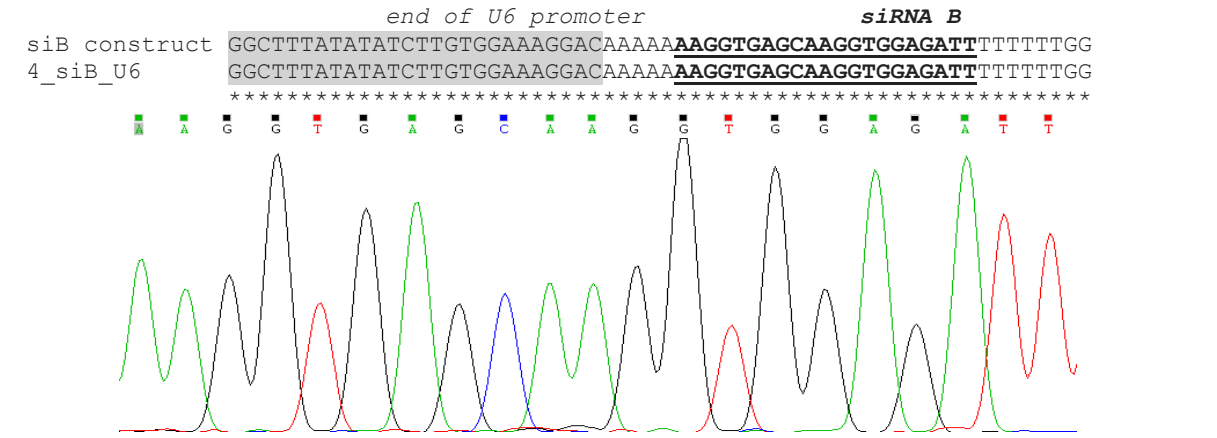

7.4 FACS data after puromycin selection

7.4.1 Backbone

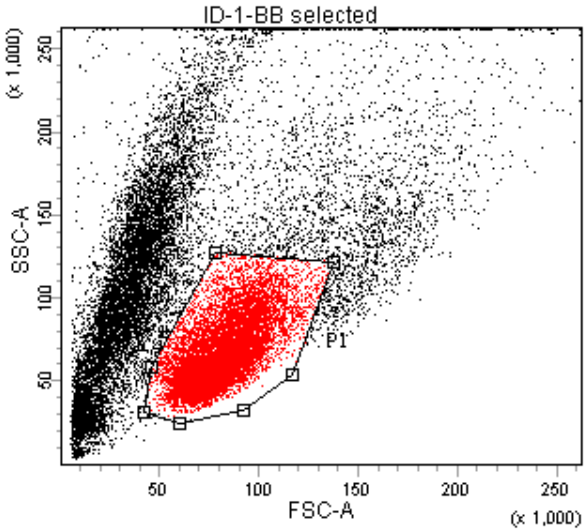

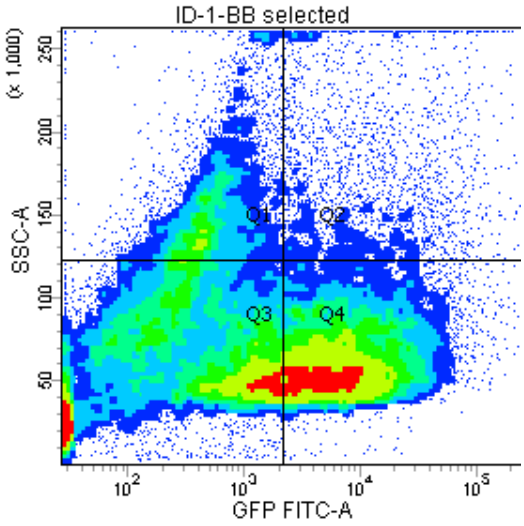

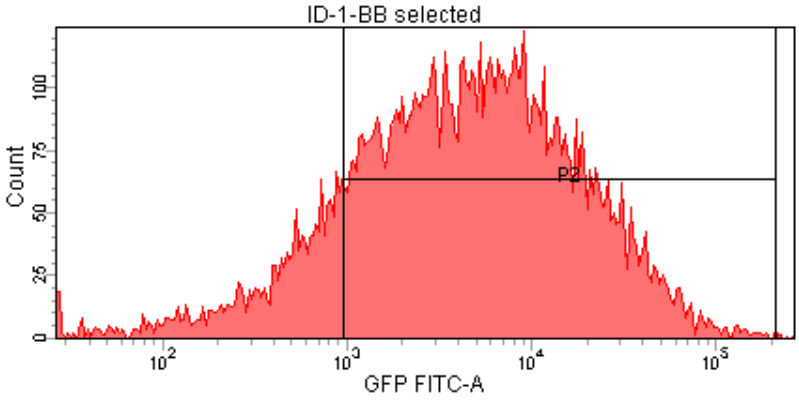

Population	#Events	%Parent	GFP FITC-A Mean
P1	10,831	46.2	10,028
P2	9,086	83.9	11,549

Tube: BB selected

Population	#Events	%Parent	%Total
All Events	23,436	####	100.0
Q1	3,443	14.7	14.7
Q2	2,263	9.7	9.7
Q3	9,741	41.6	41.6
Q4	7,989	34.1	34.1
P1	10,831	46.2	46.2
P2	9,086	83.9	38.8

7.4.2 ID-1

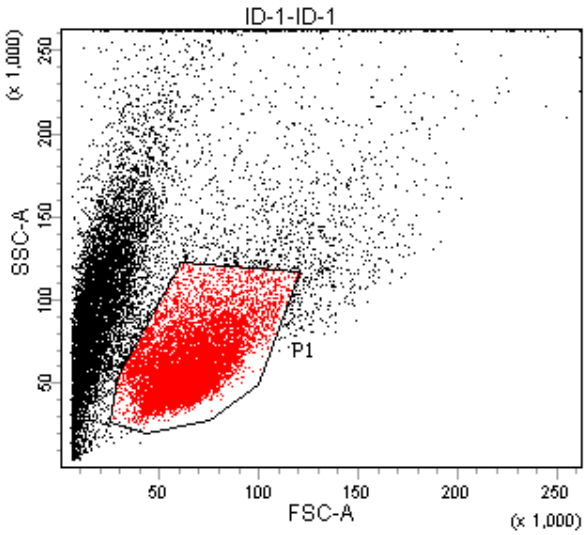

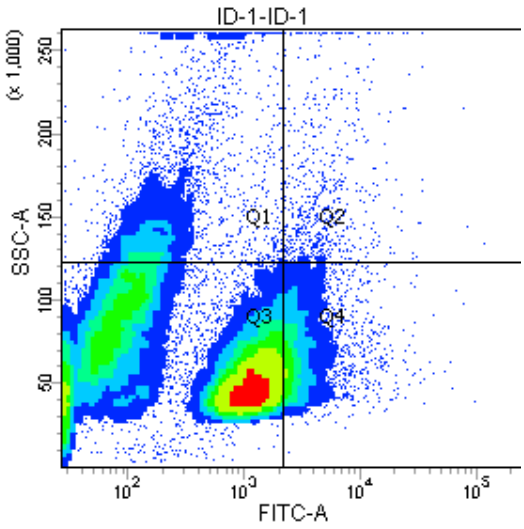

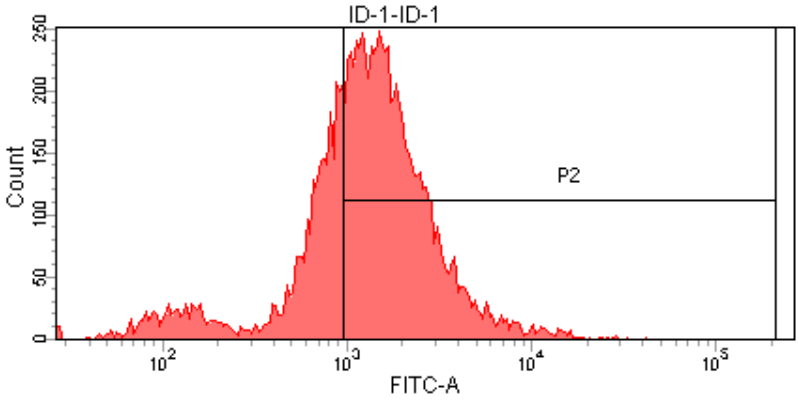

Population	#Events	%Parent	FITC-A Mean
P1	10,601	50.2	1,803
P2	7,223	68.1	2,379

Tube: ID-1

Population	#Events	%Parent	%Total
All Events	21,100	####	100.0
Q1	2,855	13.5	13.5
Q2	641	3.0	3.0
Q3	15,052	71.3	71.3
Q4	2,552	12.1	12.1
P1	10,601	50.2	50.2
P2	7,223	68.1	34.2

7.4.3 Scrambled control

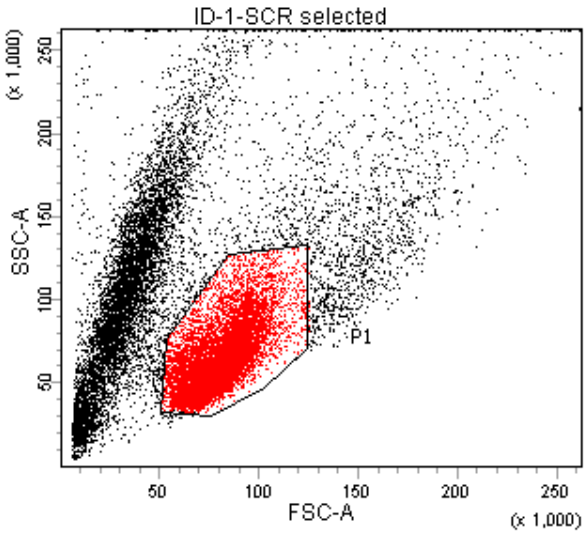

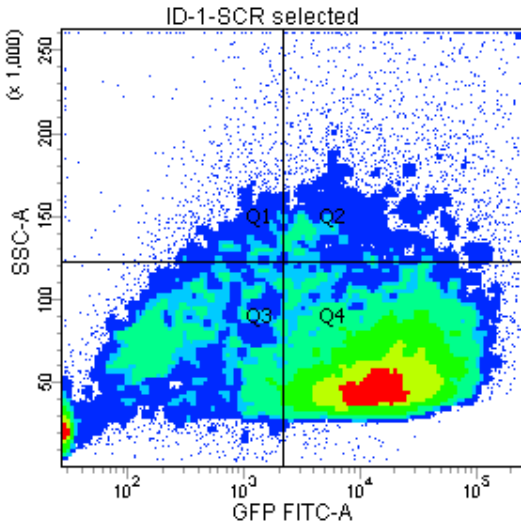

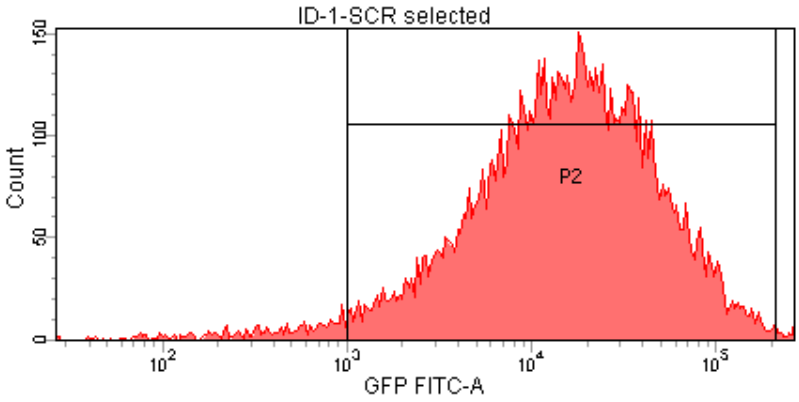

Population	#Events	%Parent	GFP FITC-A Mean
P1	10,291	53.3	25,689
P2	9,902	96.2	25,618

Tube: SCR selected

Population	#Events	%Parent	%Total
All Events	19,303	####	100.0
Q1	1,096	5.7	5.7
Q2	2,621	13.6	13.6
Q3	4,604	23.9	23.9
Q4	10,982	56.9	56.9
P1	10,291	53.3	53.3
P2	9,902	96.2	51.3

7.4.4 siA

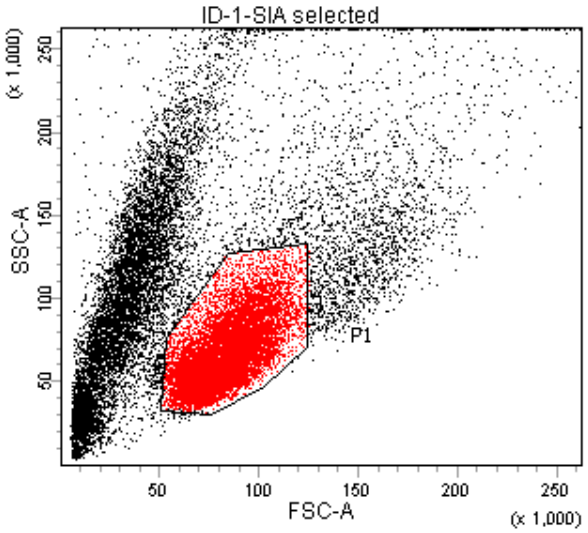

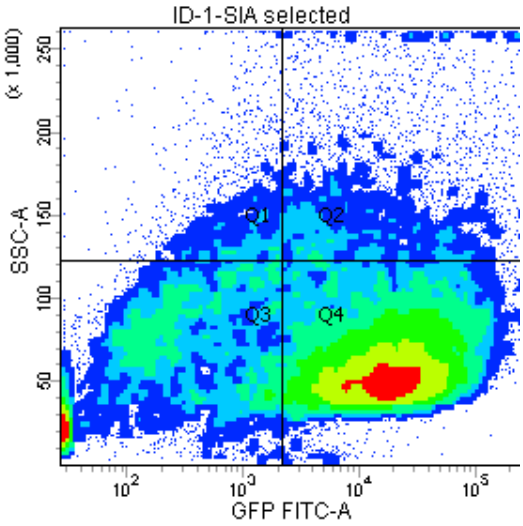

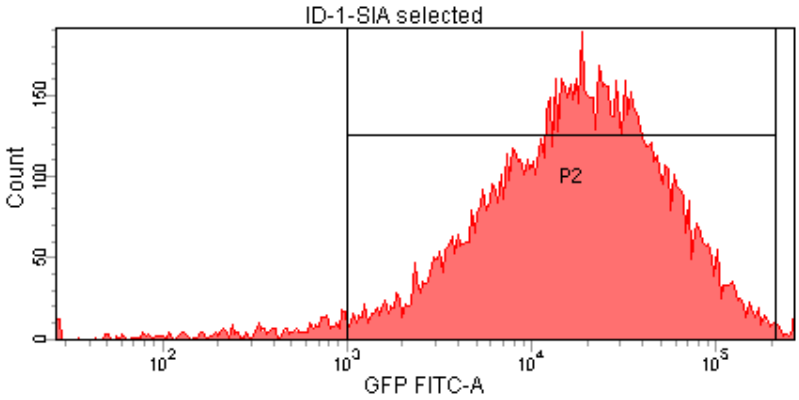

Population	#Events	%Parent	GFP FITC-A Mean
P1	12,221	51.8	28,798
P2	11,702	95.8	28,552

Tube: SIA selected

Population	#Events	%Parent	%Total
All Events	23,589	####	100.0
Q1	1,364	5.8	5.8
Q2	3,305	14.0	14.0
Q3	5,707	24.2	24.2
Q4	13,213	56.0	56.0
P1	12,221	51.8	51.8
P2	11,702	95.8	49.6

7.4.5 siB

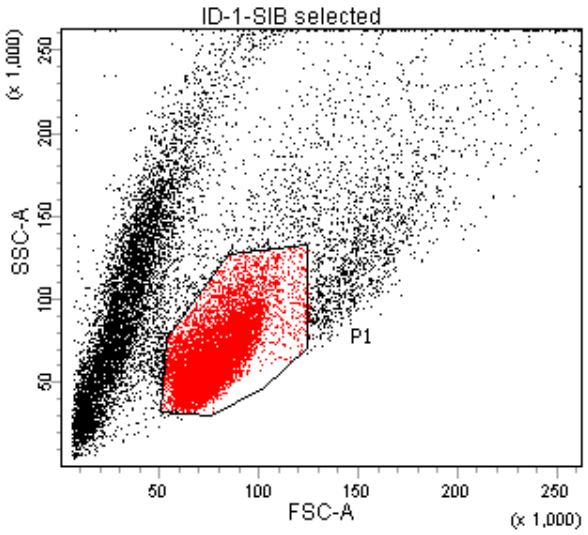

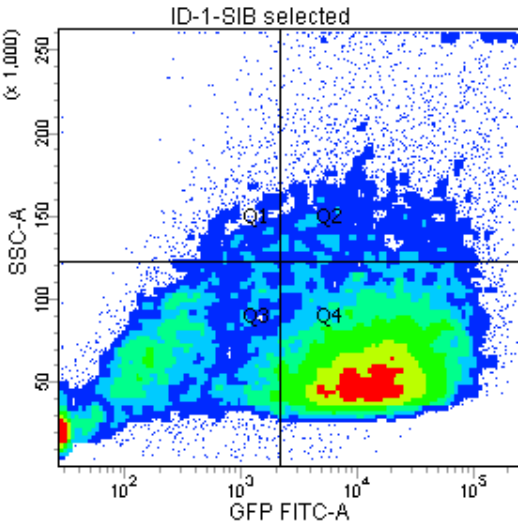

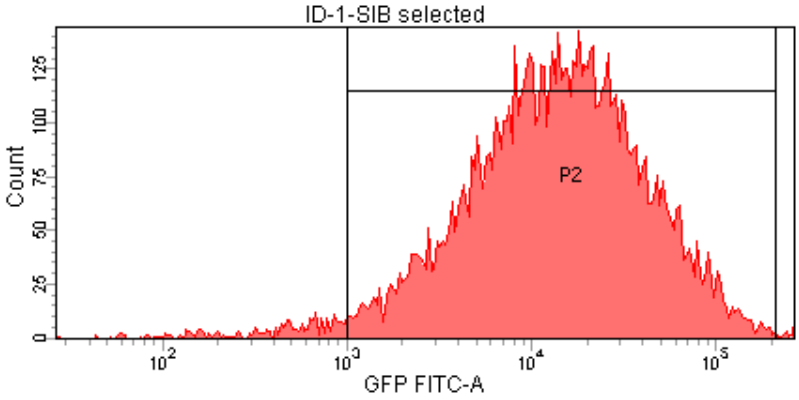

Population	#Events	%Parent	GFP FITC-A Mean
P1	9,781	52.0	22,905
P2	9,453	96.6	22,808

Tube: SIB selected

Population	#Events	%Parent	%Total
All Events	18,807	####	100.0
Q1	829	4.4	4.4
Q2	2,806	14.9	14.9
Q3	4,768	25.4	25.4
Q4	10,404	55.3	55.3
P1	9,781	52.0	52.0
P2	9,453	96.6	50.3

7.5 qPCR of ID-1

7.5.1 ID-1 overexpression, WT and BB

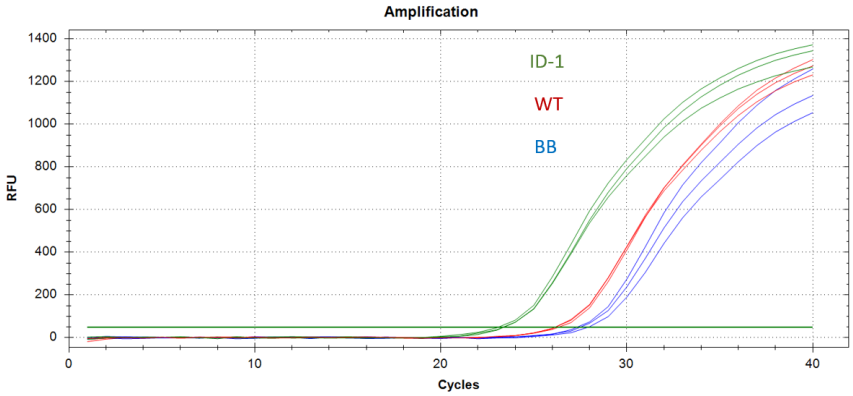

7.5.2 Silencing (scr, siA and siB)

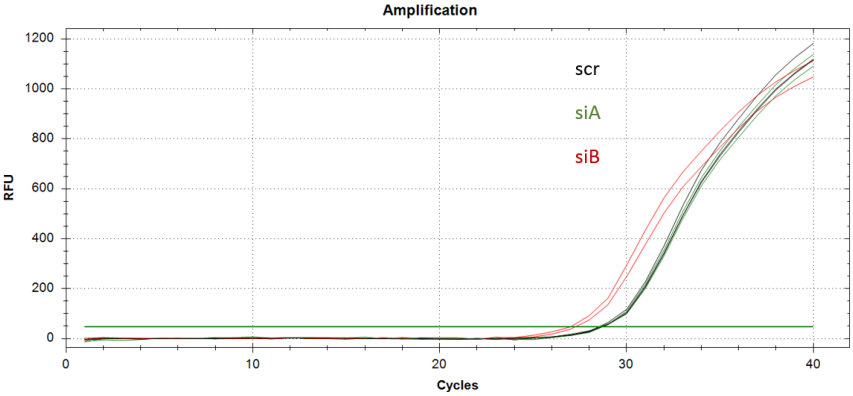

7.5.3 qPCR of β-actin

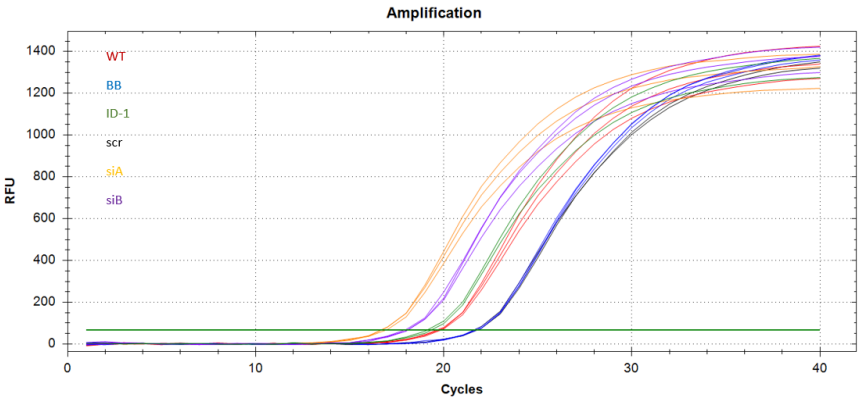

7.6 Western blot

7.6.1 BCA assay

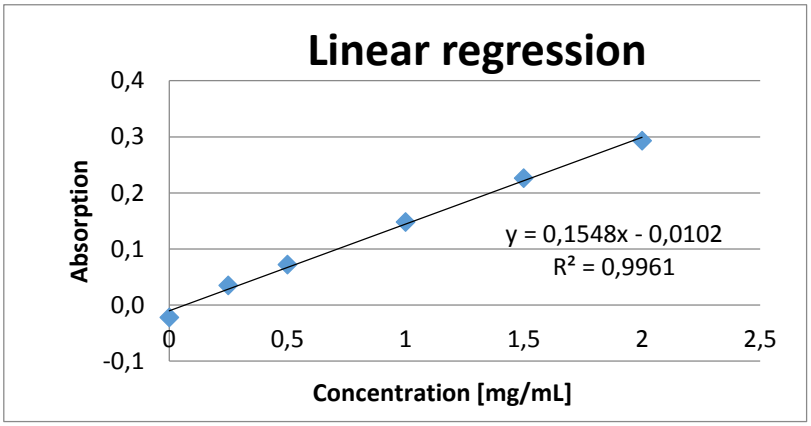

7.6.2 Western blot signals

ID-1 **β-actin**

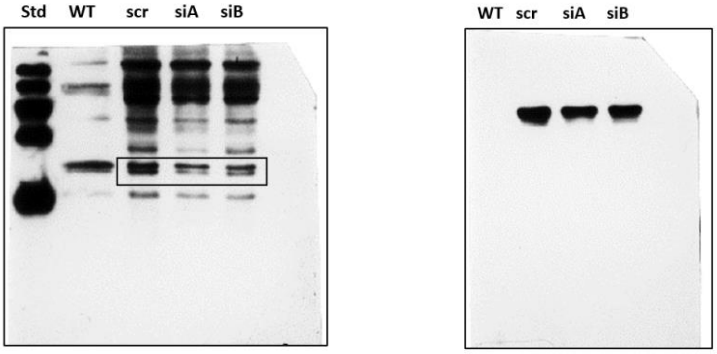

7.7 Tumor formation

7.7.1 CAM experiments

7.7.1.1 Silencing

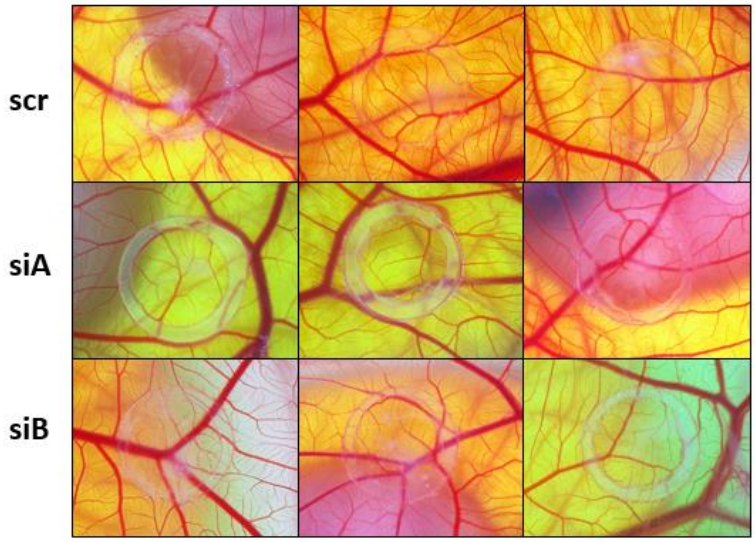

7.7.1.2 Overexpression

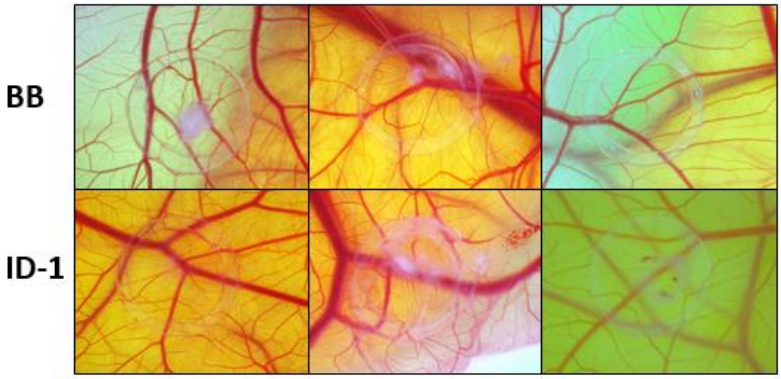

7.8 *In vitro* tumor spheroid formation

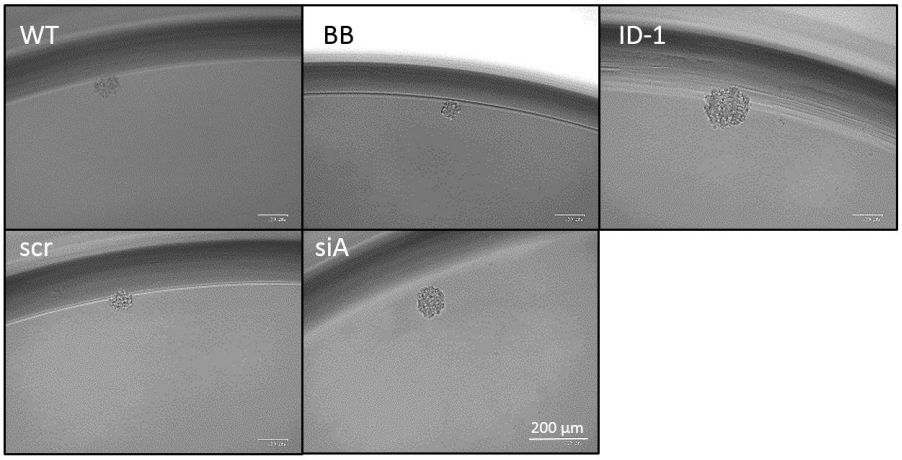

8 Conference activities

Kleinegger, F; Meier-Allard, N; Fuchs, R; Hölzl, M; Krump, C; Passegger, C; Pfragner, R; Ghaffari Tabrizi-Wizsy,N. *Cancer stem cells in small intestine neuroendocrine cell line P-STS: Isolation and molecular characterization.* 12th Annual Conference for the Diagnosis and Treatment of Neuroendocrine Tumor Diseases. 2015; -12th Annual Conference of European Neuroendocrine Tumor Society; MAR 11-13, 2015; Barcelona, SPAIN. [Poster]

Passegger, C; Kump, P; Haybäck, J; Lipp, R; Niderle, B; Pfragner, R; Sadjak, A; Schwach, G; Spindelböck, W; Ghaffari Tabrizi-Wizsy, N. *The chicken chorioallantoic membrane assay as a preclinical model for the research of rare gastrointenstinal neuroendocrine tumours.* 12th Annual Conference of European Neuroendocrine Tumor Society. 2015; -12th Annual Conference for the Diagnosis and Treatment of Neuroendocrine Tumor Diseases; MAR 11-13, 2015; Barcelona, SPAIN. [Poster]

Ghaffari Tabrizi-Wizsy, N; Passegger, CA; Kleinegger, F; Schwach, G; Schweighofer, B; Genze, F; Sadjak, A; Pfragner, R. *The Chick Embryo Chorioallantoic Membrane as a Tool to Study Medullary Thyroid Cancer.* Wiener klinische Wochenschrift, The Central European Journal of Medicine. 2014; Volume 126(Issue3):154--14th International Workshop on Multiple Endocrine Neoplasia and other rare endocrine tumors; SEPT 25-27, 2014; Vienna, AUSTRIA. [Poster]

Ghaffari-Tabrizi-Wizsy, N; Hölzl, M.; Fuchs, R; Krump, C; Pfragner, R; Kleinegger, F. *Cancer stem cells in small intestine neuroendocrine cell line P-STS: Isolation and characterisation.* Wiener Klinischer Wochenschrift, The central European Journal of Medicine. 2014; Volume 126(Issue3):154--14th International Workshop on Multiple Endocrine Neoplasia and other rare endocrine tumors; SEPT 25-27, 2014; Vienna, AUSTRIA. [Poster]

Kleinegger, F; Meier-Allard, N; Pfragner, R; Sadjak, A; Ghaffari Tabrizi-Wizsy, N. *Using alu-sequences to detect and quantify metastases of neuroendocrine tumor cells in animal xenografts.* Second International Student Congress in Austria; July 10 - 12, 2014; Graz, AUSTRIA. 2014. [Oral Communication]

Kleinegger, F; Passegger, CA; Hölzl,M ;Pfragner, R; Schwach, G; Schweighofer, B; Sadjak, A; Ghaffari Tabrizi-Wizsy, N. *The Chick Embryo Chorioallantoic Membrane as a tool to study Neuroendocrine Tumor Behavior.* 6th ÖGMBT Annual Meeting; SEPT 15-18, 2014; Vienna. 2014. [Poster]

Medical University of Graz

Cancer Stem Cells in Small Intestine Neuroendocrine Cell Line P-STS: Isolation and Molecular Characterisation

Florian Kleinegger, Nathalie Meier–Allard, Robert Fuchs, Corinna Krump,
Roswitha Pfragner and Nassim Ghaffari Tabrizi-Wizsy
Institute of Pathophysiology and Immunology, Heinrichstrasse 31a, Medical University of Graz, Austria; nassim.ghaffari@medunigraz.at

Background and Aims

Gastrointestinal neuroendocrine tumours (GI-NET) are neoplasms originating from serotonin producing enterochromaffin cells that are part of the diffuse neuroendocrine system. Although described as rare neoplasms, incidence of GI-NET has risen in the last years, survival rates remained unchanged and 60-80% of patients show metastasis at time of diagnosis. While surgery remains the only curative treatment, less than 15% of all patients have likelihood for a curative intervention. Cancer stem cells (CSCs) represent a small subpopulation of tumour cells responsible for invasive tumour growth and chemotherapeutic resistance. Their role in neuroendocrine tumourigenesis and metastasis remains uncertain.[1]

We hypothesised that
P-STS contains a subpopulation of neuroendocrine cancer stem cells

Materials and Methods

3D spheroid culture: P-STS cell line was grown as 3D spheroids by cultivating 7500 cells in ultra low-adhesion round bottom 96-well plates for 5 days.
Cancer stem cell marker: Aldehyde dehydrogenase (ALDH) activity was detected and cells have been isolated using the Aldefluor kit. Membrane-bound CSC marker (CD133, CD15, CD44, CD117 and CD24) were analysed by flow-activated cell sorting (FACS). Further potential CSC markers (Nestin, Musashi-1, BMI1, Id-1, Oct-4, NES, CD15, CD133, CD24, CD117, Sox2) were analysed by reverse transcriptase-PCR.
Chorioallantoic membrane assay: Grafted 15000 P-STS cells or two (containing 7500 cells each) P-STS spheroids at day 10 of the chicken embryonic development on the CAM. After 3 days of incubation further histological examination was done.

Results

Stem cell genes expression

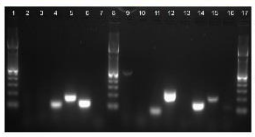

Figure 1: Analysis of stem cell markers RT-PCR.
1,8,17 Ladder 100bp; 2 PDPN; 3 CD15 4 CD133; 5 CD24; 6 CD117; 7 ABCG2; 9 NES; 10 ALDH1; 11 MSI1; 12 BMI1; 13 SOX2; 14 Id1; 15 OCT4; 16 Nanog

Spheroid Formation

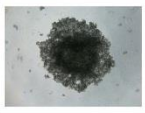

Figure 3: Spheroid formation. 7500 P-STS cells were cultivated in 96 well ultra low adhesion round bottom plates for 5 days, prior grafting on CAM

Aldefluor assay

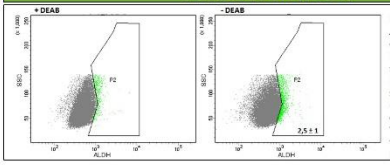

Figure 2: Identification of ALDH⁺ cells in the P-STS cell line.
FACS analysis of P-STS stained by ALDEFLUOR™ Kit. Dot-plots show ALDH⁺ subpopulations in "-DEAB" (right panel) and the negative control, "+DEAB" (left panel). "+DEAB" was used for gaiting the ALDH expressing population (-DEAB).

CSC surface markers

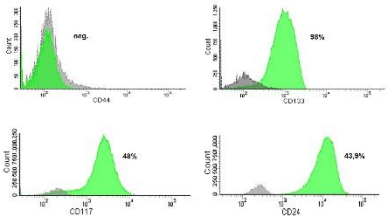

Figure 4: Expression of characteristic CSC surface markers in P-STS single cells assessed by flow cytometry.
Cells were stained with BV- and PE-conjugated monoclonal antibodies against CD117, CD133, CD24 and CD44. The histograms from FACS show the percentage of the positive cells (green) and the isotype control (grey). P-STS single cells were 98% CD133, 43,9% CD24 and 48% CD117 positive. CD44 was negative.

Comparison of P-STS 2D and 3D on CAM

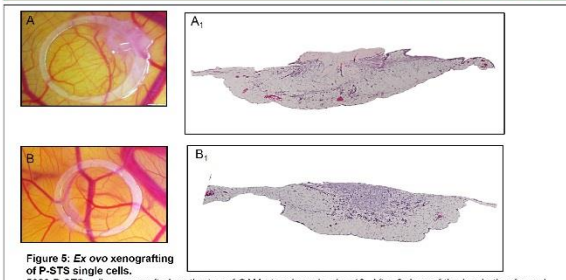

Figure 5: *Ex ovo* xenografting of P-STS single cells.
5000 P-STS cells were grafted on the top of CAM at embryonic day 10. After 3 days of the incubation formed tumors were collected.
A: Macroscopic picture (top view) of tumor development with Matrigel™ after 3 days of incubation.
A_1: Histologic (H&E) analysis of tumor with Matrigel™ collected 3 days after implantation
B: Macroscopic picture (top view) of tumor development without Matrigel™ after 3 days of incubation
B_1: Histologic (H&E) analysis of tumor without Matrigel™ collected 3 days after implantation

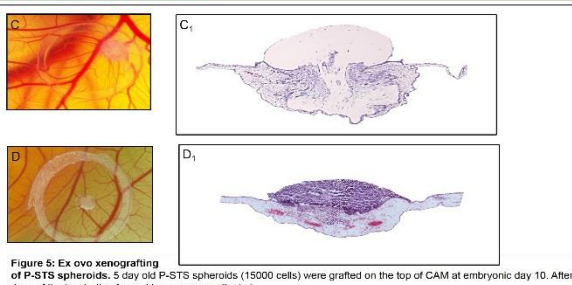

Figure 5: Ex ovo xenografting of P-STS spheroids. 5 day old P-STS spheroids (15000 cells) were grafted on the top of CAM at embryonic day 10. After 3 days of the incubation formed tumors were collected.
C: Macroscopic picture (top view) of tumor development with Matrigel™ after 3 days of incubation.
C_1: Histologic (H&E) analysis of tumor with Matrigel™ collected 3 days after implantation
D: Macroscopic picture (top view) of tumor development without Matrigel™ after 3 days of incubation
D_1: Histologic (H&E) analysis of tumor without Matrigel™ collected 3 days after implantation

Conclusion

- Characteristic CSC markers are expressed in P-STS cell line
- Some surface markers are expressed
- P-STS cells contain a ALDH⁺ population
- CAM assay is an excellent alternative animal study
- CAM model system is suitable for invasion studies
- Spheroids are more invasive than single cells

References

1. Pfragner, R. *et al.* Establishment and characterization of three novel cell lines - P-STS, L-STS, H-STS - derived from a human metastatic midgut carcinoid. *Anticancer Res.* **29**, 1951-1961 (2009).

COMPREHENSIVE CANCER CENTER GRAZ Krebszentrum
Medizinische Universität & UKH-Univ. Klinikum

ENETS European Neuroendocrine Tumor Society

GJKGEP NETZWERK

SFLA

Contact: nassim.ghaffari@medunigraz.at

The Chick Embryo Chorioallantoic Membrane as a tool to study Neuroendocrine Tumor Behavior

Medical University of Graz

Florian Kleinegger[1], Christina A. Passegger[1], Marlies Hölzl[1], Roswitha Pfragner[1], Gert Schwach[1], Bernhard Schweighofer[2], Anton Sadjak[1] and Nassim Ghaffari Tabrizi-Wizsy[1]

[1] Institute of Pathophysiology and Immunology, Heinrichstrasse 31a, Medical University of Graz, Austria;
[2] Department of Dermatology, SERD, Währingergürtel 18-20, Medical University of Vienna, Austria;

BACKGROUND AND AIM

Neuroendocrine tumors (NET) arise from the diffuse neuroendocrine system. They are rare tumors and show poor response to conventional therapy. The tumors occur in the whole body including pancreas, skin, thyroid, intestine and lung, respectively. The chick chorioallantoic membrane (CAM) assay is a well-established model, which allows *in vivo* studies of tumor growth, angiogenesis and metastasis. CAM, a well vascularized extra-embryonic tissue, provides grafted tumor cells with a physiological supply of nutrients, cytokines and vascularization. Beyond that, at this stage the chick immune system is not fully developed and the conditions for rejection have not been established. CAM can also be used to develop antitumoral and antiangiogenic drugs. Subject of this study were different NET cell lines (including medullary thyroid carcinoma, small intestine-NET and xenografts of tumor tissue) placed on CAM for 72-168 hours. The xenografts were excised and analyzed histologically.

Question: Is the CAM model suitable for neuroendocrine tumor cell lines studies?

MATERIALS AND METHODS

CAM assay: Fertilized, white Leghorn eggs were incubated for 3 days at 37°C and 60% humidity. For better access to the CAM the eggs were cracked and cultivated in dishes. On day 10 of the chicken embryo development, the onplants were performed using between 1.5 x10^4 and 1 x10^6 cells per onplant, mixed with Matrigel™ and a silicone ring bordering the cell suspension. Further, the chick embryos were incubated for a maximum of another 7 days and the morphological tumor development was documented microscopically. After the incubation, the onplants were excised, dehydrated and paraffin embedded or prepared for cryo sectioning. The paraffin embedded specimen were analyzed histologically via hematoxylin and eosin staining and immunohistochemistry.

RESULTS

Figure 1: P-STS cell line is highly angiogenic and forms macroscopically visible tumors. The development of 1 x10^6 P-STS (SI-NET) cells grafted on the CAM over one week leads to the formation of a macroscopically visible tumor, approximately 2 mm in diameter. The angiogenetic ability of these cells is marked by the increasing number and thickness of blood vessels surrounding the tumor.

Figure 2: eGFP tagged P-STS cells show invasive behavior on the CAM. After grafting 1 x10^6 eGFP tagged P-STS cells and incubation for 4 days, they show invasion of vessels near the tumor (arrows), detected by fluorescence microscopy.

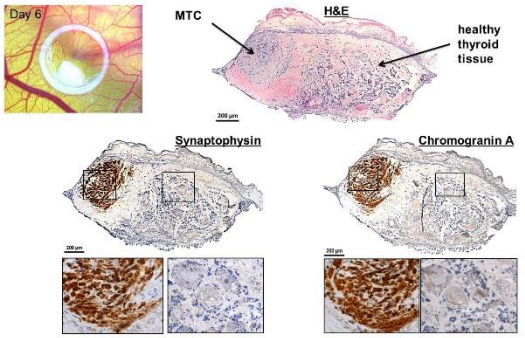

Figure 3: MTC primary tumor tissue cultivated on CAM grows well and retains specific tumor markers. Tumor tissue cultivated on the CAM for 6 days. Subsequent histological analysis showed that the tumor tissue was positive for tumor markers synaptophysin and chromogranin A, whereas surrounding tissue shows non-pathological thyroid morphology.

CONCLUSIONS

- ✓ CAM assay is an excellent alternative to animal studies
- ✓ NET cell lines grow well and invasive on CAM
- ✓ CAM model system is suitable for NET characterization studies
- ✓ NET tissue xenografts grow well on CAM
- ✓ CAM assay is cost effective, quick and leads to reproductive results

contact: nassim.ghaffari@medunigraz.at; florian.kleinegger@medunigraz.at

ÖGMBT 2014

The Chick Embryo Chorioallantoic Membrane as a Tool to Study Medullary Thyroid Cancer

Medical University of Graz

Nassim Ghaffari Tabrizi-Wizsy[1], Christina Angelika Passegger[1], Florian Kleinegger[1], Gert Schwach[1], Bernhard Schweighofer[2], Felicitas Genze[3], Anton Sadjak[1], Roswitha Pfragner[1]

[1] Institute of Pathphysiology and Immunology, Heinrichstraße 31a, Medical University of Graz, Austria;
[2] Department of Dermatology, SERD, Währingergürtel 18-20, Medical University of Vienna, Austria;
[3] ILM, Helmholtzstraße 12, Ulm University, Germany

BACKGROUND AND AIMS

The chick chorioallantoic membrane (CAM) assay is a well-established model, which allows *in vivo* studies of tumor growth, angiogenesis and metastasis. CAM, a well vascularized extra-embryonic tissue located underneath the eggshell, provides tumor cells with a physiological supply of nutrients, cytokines and vascularization as the natural tissue site. Beyond that, at this stage the immune system of the chick is not fully developed and the conditions for rejection have not been established[1-2].

MATERIALS AND METHODS

Fertilized Leghorn eggs were incubated at 37°C and 60% humidity. On day 10 of embryonic development onplants with $1x10^6$ medullary thyroid cancer (MTC) cells or tumor tissue were grafted on the CAM of *ex ovo* cultivated embryos. Tumor formation was allowed to happen for 3-6 days before tumors with the CAM were excised and fixed in 4% paraformaldehyde. Paraffin embedded specimens were processed for histological examination with hematoxylin/eosin (H&E) staining and immunohistochemistry, respectively.

RESULTS

Development of different MTC cell lines on CAM

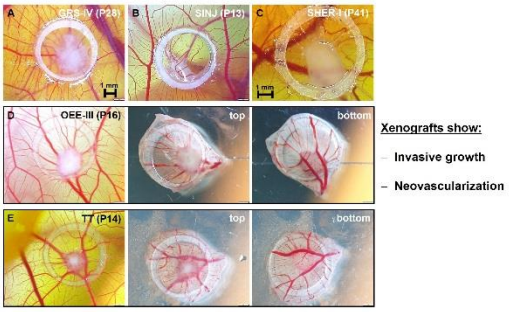

Figure 1: MTC cell lines grafted on the CAM form solid tumors. Xenografts of MTC cell lines GRS-IV (**A**), SINJ (**B**), SHER-I (**C**), OEE-III (**D**) and TT (**E**), respectively, form well vascularized tumors on CAM.

MTC tumor tissue grafted on CAM

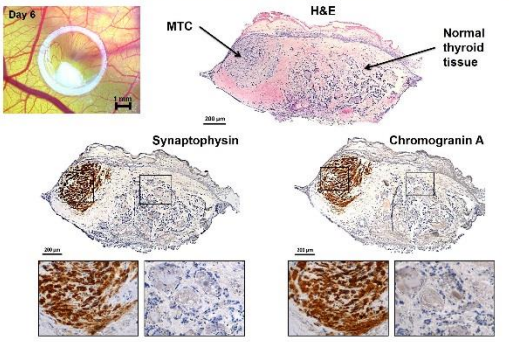

Figure 3: MTC primary tumor tissue grafted on the CAM retained to express specific tumor markers. Tumor tissue grown on the CAM for 6 days (top left corner). Subsequent histological analyses showed that the tumor tissue was positive for tumor markers Synaptophysin and Chromogranin A, whereas surrounding tissue showed non-pathological thyroid morphology.

Histological examination of MTC-SK onplant

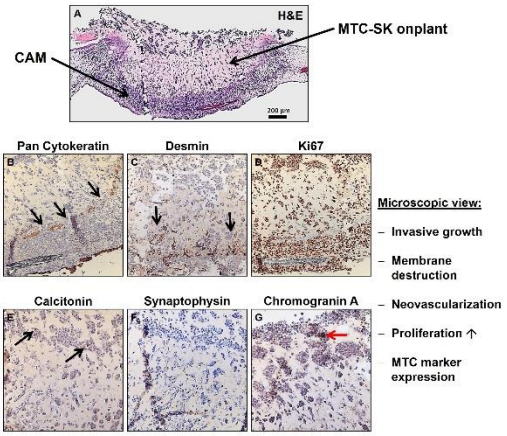

Figure 2: Histological examination of MTC-SK onplant. MTC-SK cells (P350) seeded on the CAM grew dense (**A**) and were highly proliferative (Ki67 positive, **D**). Moreover, the cells grew invasive and destructed the basal membrane of the CAM (**B**, arrows). The xenograft was well vascularized by increased numbers of blood vessels that occurred at the onplant-CAM-border and also penetrated the xenograft tissue (**C**, arrows). MTC-SK cells still expressed specific biomarkers such as Calcitonin and Chromogranin A (**E, G**, arrows).

CONCLUSION

- ✓ CAM assay is an excellent alternative to animal studies
- ✓ MTC cell lines form macroscopically visible tumors already after 72h
- ✓ MTC onplants are highly proliferative, grow invasive and show neovascularization
- ✓ MTC tissue xenografts grow well on CAM and still express specific tumor markers
- ✓ CAM assay is cost effective, quick and leads to reproducible results

REFERENCES

[1] Kain, K. H. et al. *Dev. Dyn.* **243**: 216-228 (2014).
[2] Deryugina E.I. & Quigley J.P. *Histochem Cell Biol.* **130**(6): 1119-1130 (2008).

World Men 2014 - Vienna

Contact information:
nassim.ghaffari@medunigraz.at
christina.passegger@medunigraz.at